CSST
Chair of Computational Science and Simulation Technology

Leibniz Universität Hannover

Multiscale Modelling and Optimization of Flexoelectric Nano Structures

Xiaoying Zhuang

Faculty of Mathematics and Physics
Leibniz University Hannover
Hannover Center for Optical Technology

Jan 20 2022

Piezoelectricity V.S. flexoelectricity

CSST Chair of Computational Science and Simulation Technology

Centrosymmetric crystals

All type of materials

Initial state

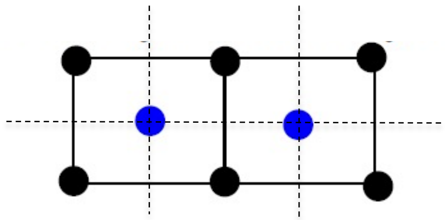

Deformed state
Uniform strain

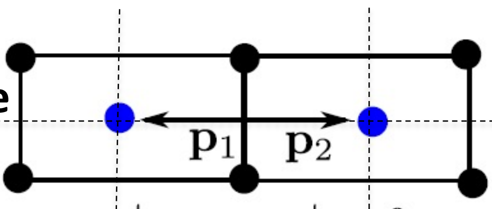

$|\mathbf{p}_1 - \mathbf{p}_2| = 0$

$$P^{\alpha} = \boxed{\mu^{\alpha\beta\gamma\delta} \frac{\partial \epsilon^{\gamma\delta}}{\partial x_{\beta}}} + \boxed{d^{\alpha\beta\gamma} \epsilon^{\beta\gamma}}$$

Flexo **Piezo**

Deformed state
Strain gradient

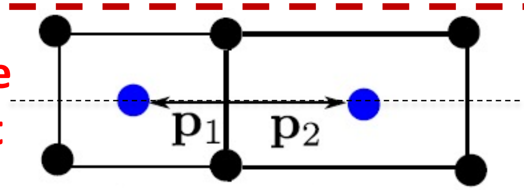

$|\mathbf{p}_1 - \mathbf{p}_2| > 0$

Flexo

Non-centrosymmetric crystals

Quartz, ZnO, Sucrose, Lead titanate, bone, DNA

Initial state

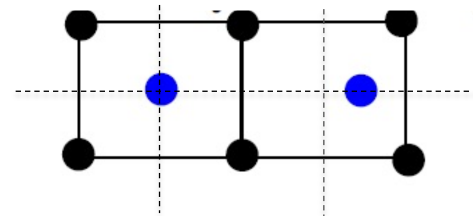

Deformed state
Uniform strain

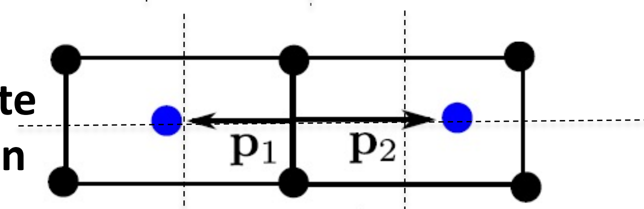

$|\mathbf{p}_1 - \mathbf{p}_2| > 0$

Piezo

Deformed state
Strain gradient

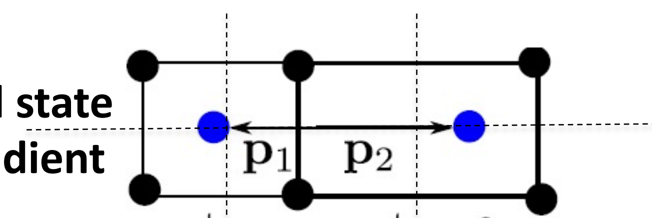

$|\mathbf{p}_1 - \mathbf{p}_2| > 0$

Flexo + Piezo

Flexoelectricity: strain engineering

Inhomogeneous deformation → Strain engineering

WHAT is FLEXOELECTRICITY?

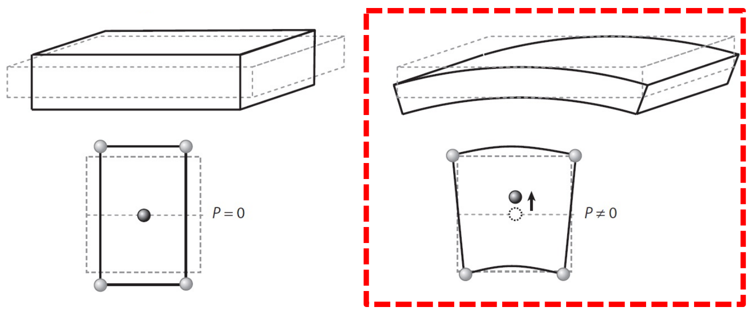

$$P_3 = \mu_{12}\boxed{\frac{\partial \varepsilon_{11}}{\partial x_3}}$$

Gradient of strain!

Bending, crumpling, torsion…

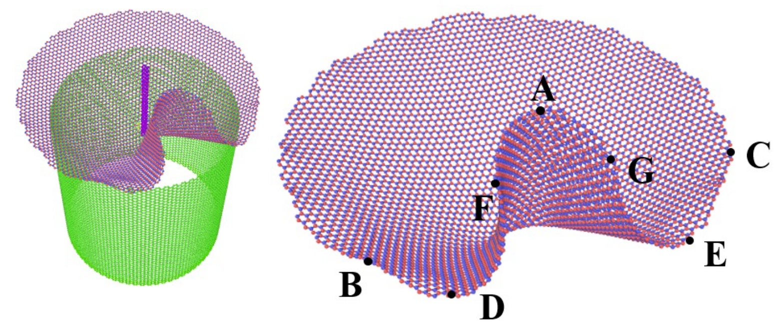

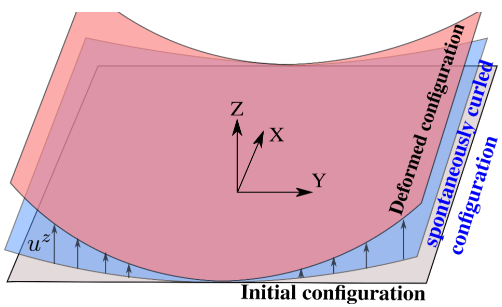

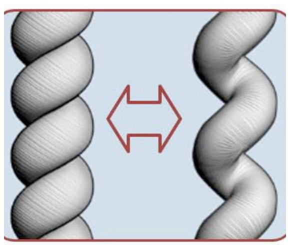

Akinwande et al., Nat. Comm., 2014; Wang et al., Phys. Rev. B., 2019; Jiang et al. Nano Energy, 2013; Kvashnin et al., J. Phys. Chem. Lett., 2018; Kim et al., Science, 2017.

Where does flexoelectricity exist?

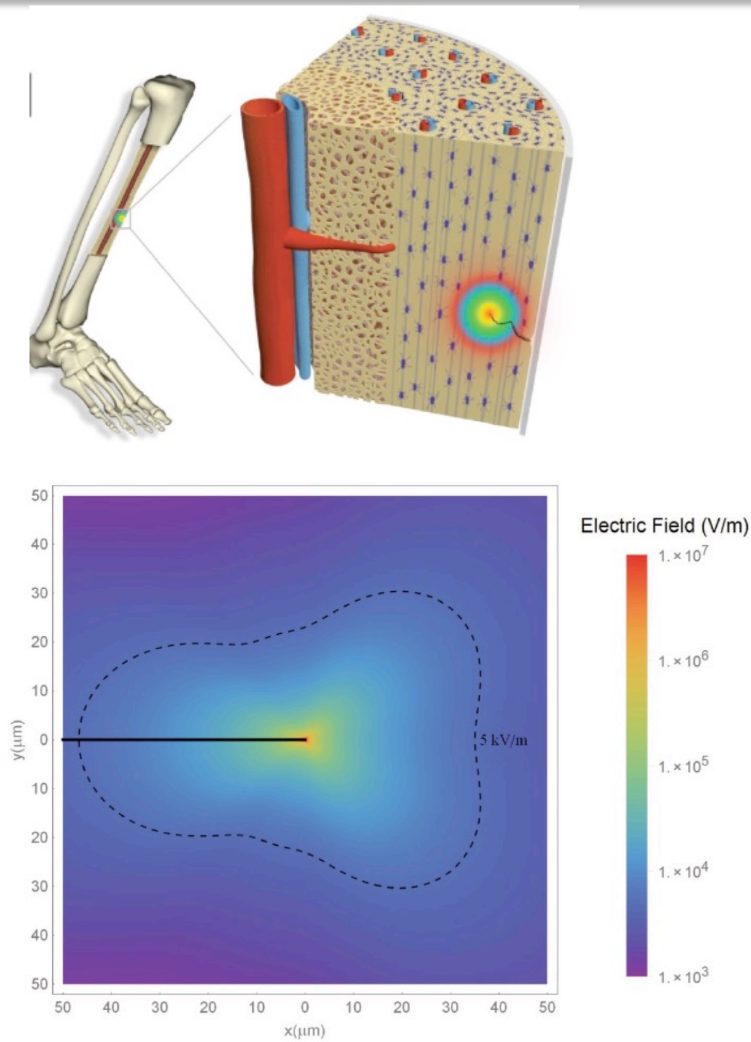

Flexoelectricity around a microcrack bone model

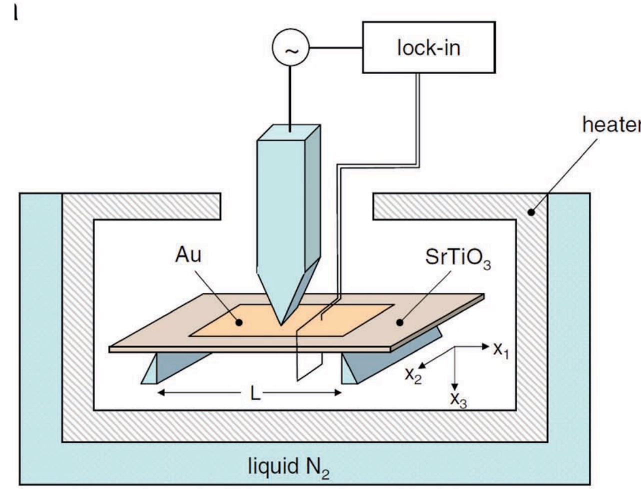

Crystalline material e.g. STO by bending induced flexoelectricity

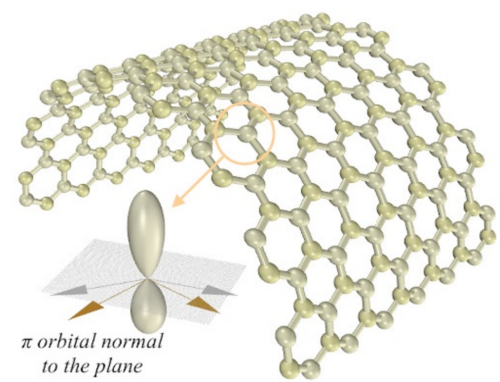

In graphene by breaking symmetry

Vasquez-Sancho et al., Adv. Mater. 2018, 30, 1705316; Zubko et al., Phys. Rev. Lett., 2007, 99, 167601

Unsolved issues and challenges

- Flexoelectric parameters are unclear
- Many phenomena are not understood: surface piezo, surface flexo, free charge carriers…
- *HOW* to engineer and optimize flexoelectricity?

Lack of physical model and simulation tool!

Inconsistent results?

	Barium Titanate (BTO)	
	μ_{11} (nC/m)	μ_{12} (nC/m)
Cross [Experiment]	---	9508~10980
Sharma [Lattice dynamics]	0.15	-5.46
Tao [First principle]	-0.36	1.6
Vanderbilt [First principle]	-334.3	13.8

Overview

- **Atomic-scale** model of flexoelectric materials
- **Nano-continuum scale** model of flexoelectric structures
- **Microscale** model of flexoelectric composites
- **Macroscale** application with phonic topological insulator

Atomistic BTO-Core shell model

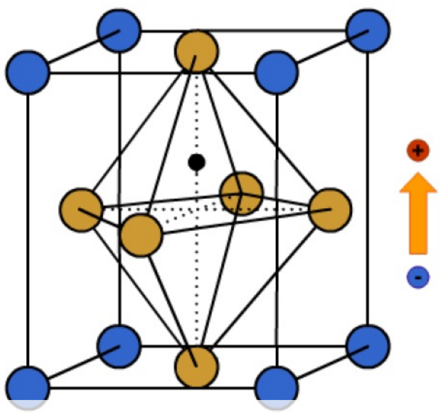

BTO model

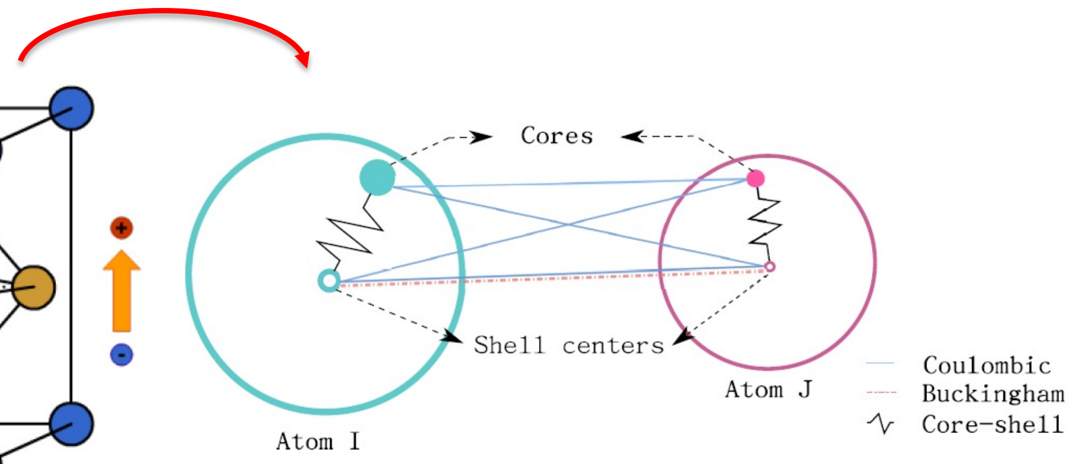

Buckingham short range potential

Long range Coulombic potential

$$E_{total}(r_{ij}) = \sum_{i=1}^{N} \sum_{i \neq j} \left\{ A_{ij} \exp\left(\frac{r_{ij}}{\rho}\right) - \frac{B_{ij}}{r_{ij}^6} \right\} + \frac{q_i\, q_j}{4\pi\varepsilon_0 r_{ij}}$$

$$+ \frac{1}{2} k_2 \left|\mathbf{r}_{ij}^2\right| + \frac{1}{24} k_4 \left|\mathbf{r}_{ij}^4\right|$$

BTO atomistic model

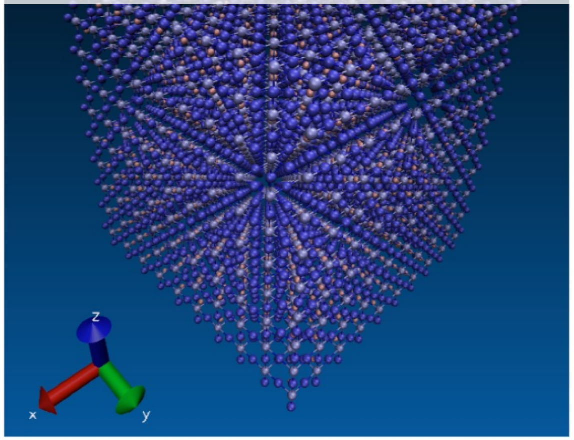

Lattice change over temperature

Results

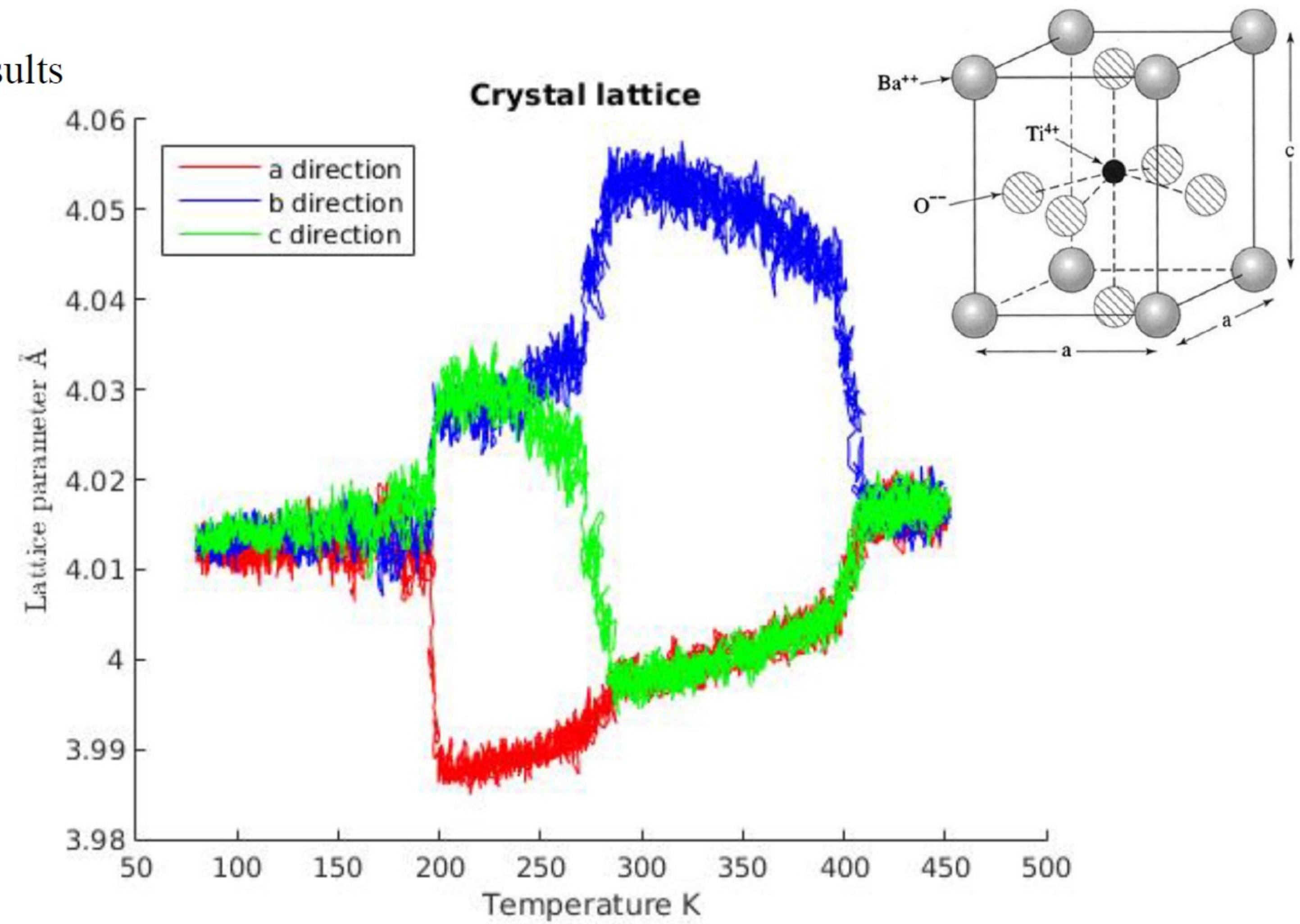

B. He, B. Javvaji and X. Zhuang. Size dependent flexoelectric and mechanical properties of barium titanate nanobelt: a molecular dynamics study. Physica B: Condensed Matter, doi.org/10.1016/j.physb.2018.01.031, 2018.

Extraction of flexo parameters

$$\delta^{long}(z) = \frac{\epsilon_{max} h}{2\pi} \sin(\frac{2\pi z}{h}),$$

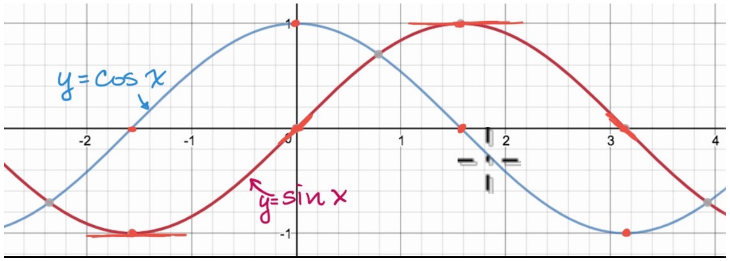

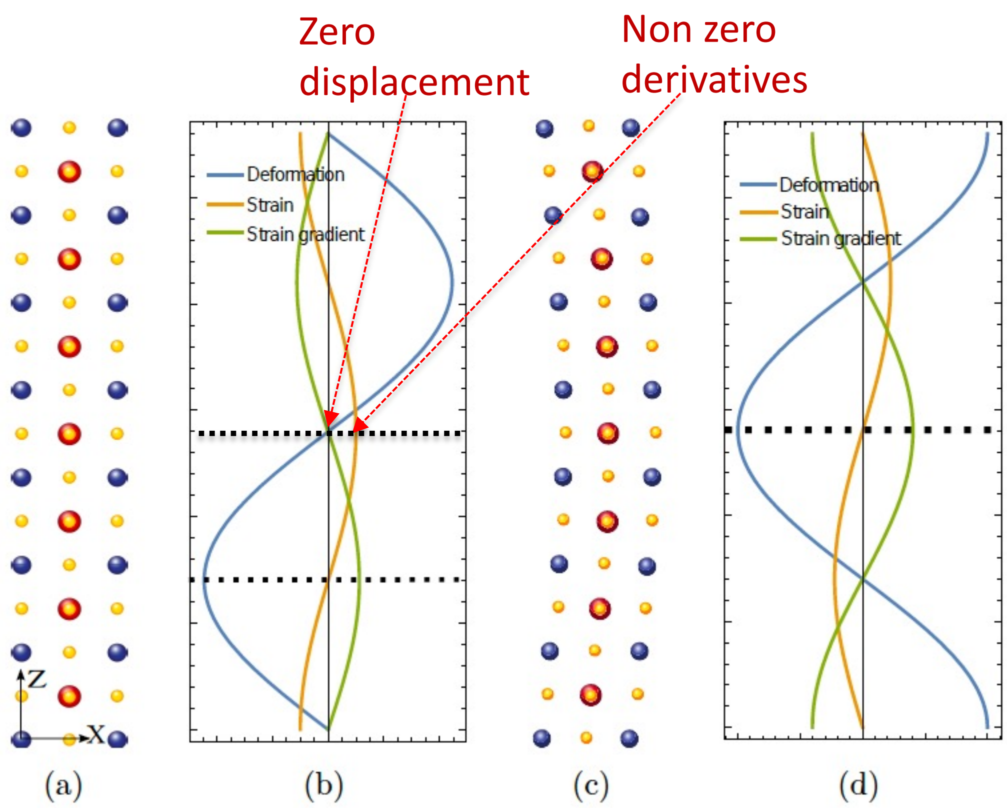

Imposition of sinusoidal boundary conditions to exclude piezoelectricity

Size effects of BTO

Size dependent Young's modulus (BTO nano-beam with different cross section size)

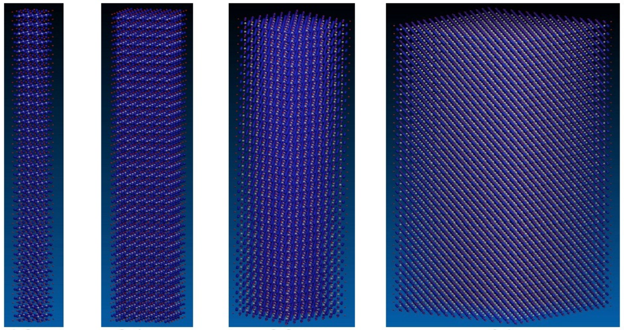

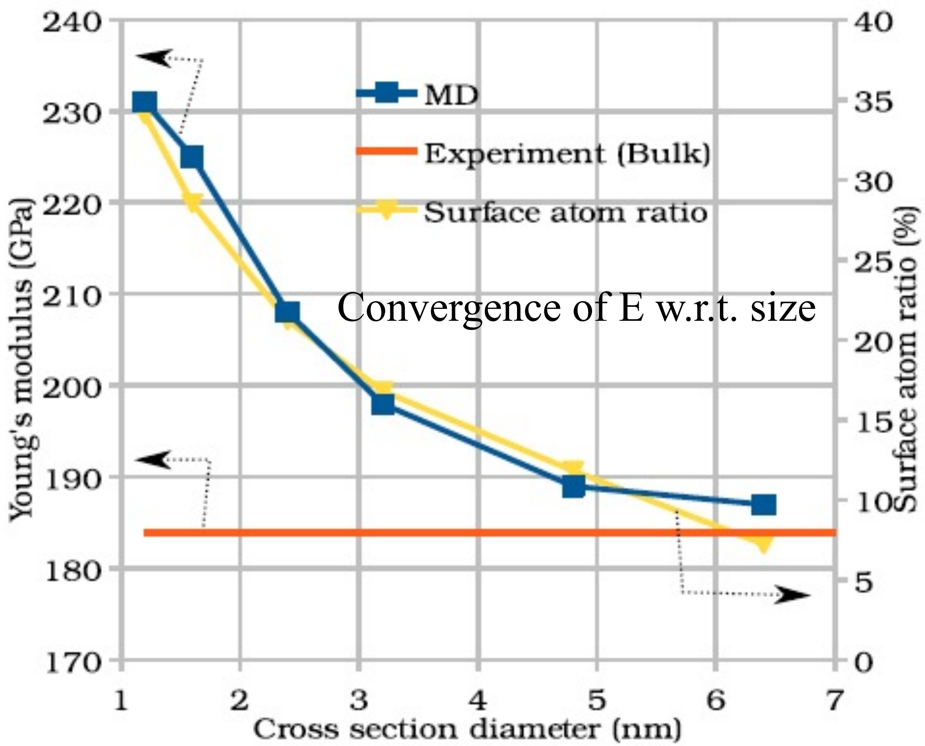

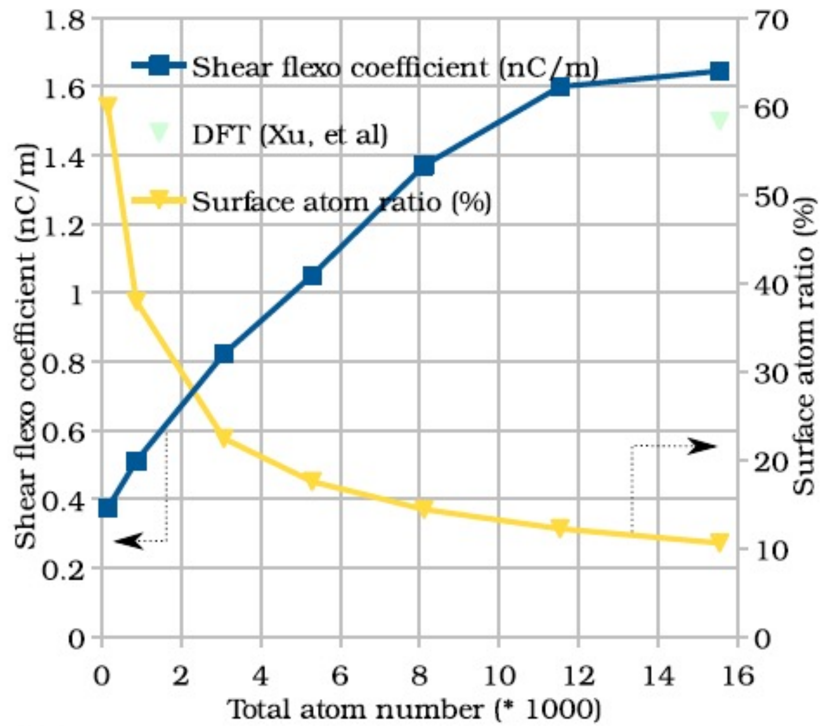

B. He, B. Javvaji and X. Zhuang. Size dependent flexoelectric and mechanical properties of barium titanate nanobelt: a molecular dynamics study. Physica B: Condensed Matter, doi.org/10.1016/j.physb.2018.01.031, 2018.

Flexoelectricity in 2D materials

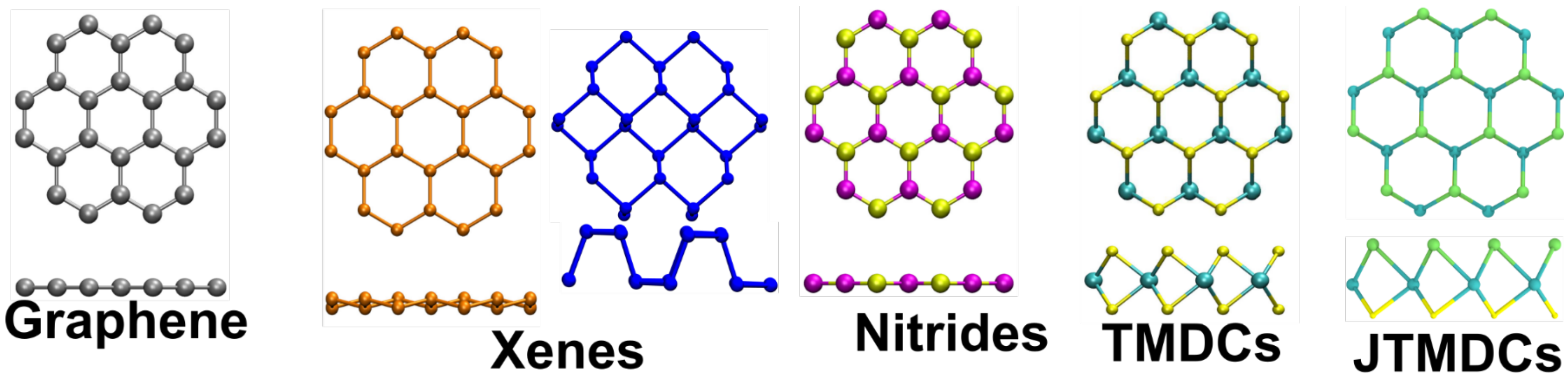

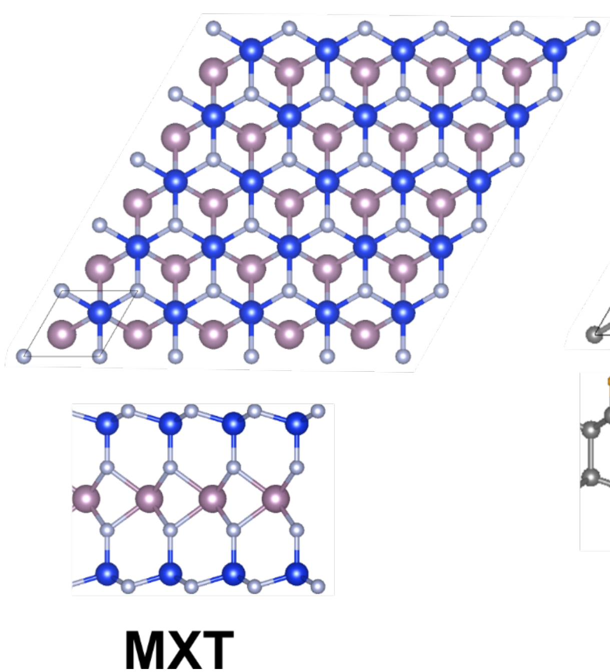

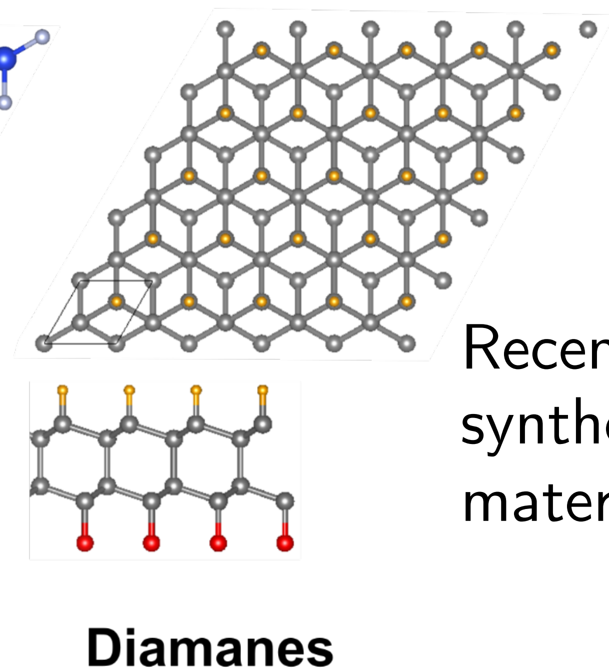

Recent experimentally synthesized 2D materials

Classical method: Difficulty

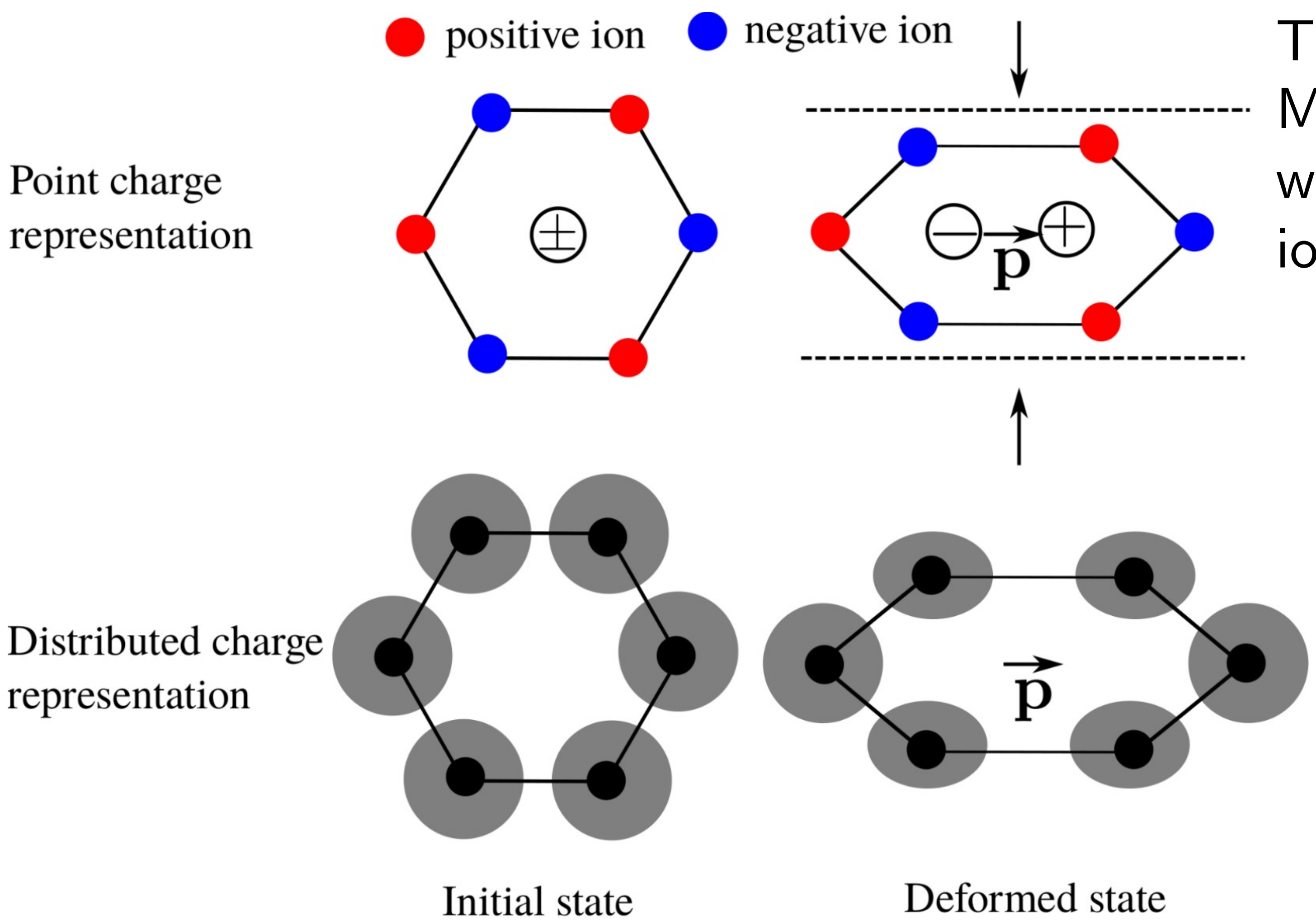

The previous MD methods works well with ionic systems

They fail to investigate the systems with charge distributed (covalent or metallic systems)

Classical method: Difficulty

We need a model that can handle

- Non-periodicity
- Dynamical changes in charges and dipoles
- Both small and large deformations
- Realistic loading conditions
- Works for any system (irrespective of bonding nature)

We developed a scheme that estimates the charges and dipoles (CD model) during the MD time integration

Charge dipole model for graphene

The total atomic interaction energy of Graphene system consist of short range and long range interaction.

$$E = E^{\mathrm{AIREBO}} + \underline{E^{\mathrm{q\text{-}q}} + E^{\mathrm{q\text{-}p}} + E^{\mathrm{p\text{-}p}} + E^{\mathrm{ext}}}$$

short range

long range (charge-dipole)

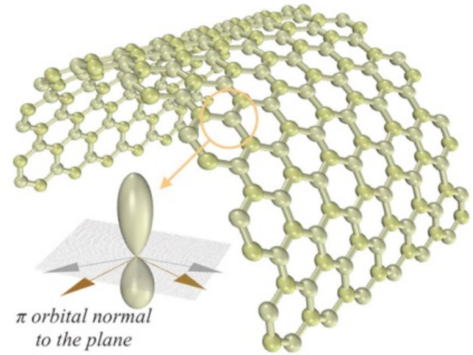

Charge-dipole scheme

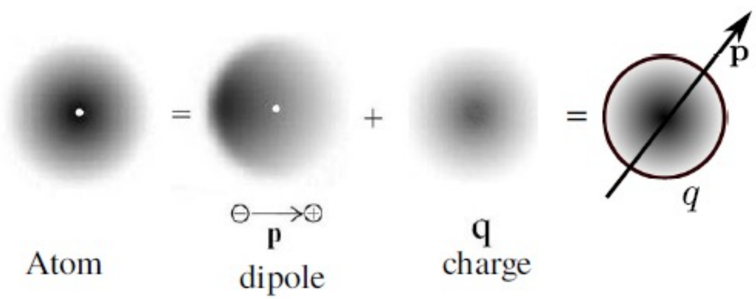

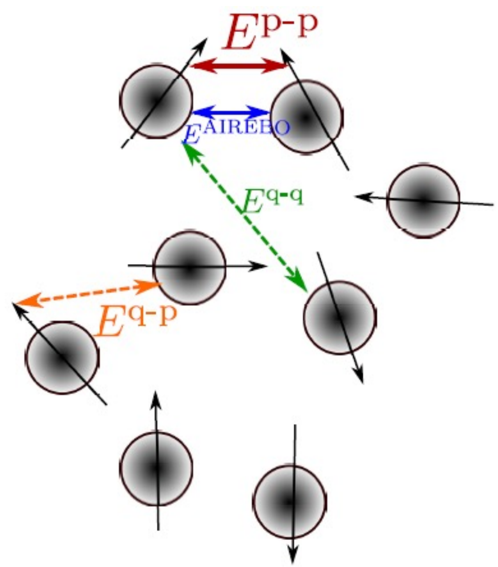

B. Javvaji, B. He and X. Zhuang. The generation of piezoelectricity and flexoelectricity in graphene by breaking the materials symmetries. Nanotechnology, 29: 225702 , 2018.

Charge dipole model for graphene

Governing equation

$$m_i \ddot{\mathbf{r}}_i = -\frac{\partial E^{\text{Short-range}}}{\partial \mathbf{r}_i} - \frac{\partial E^{q-q}}{\partial \mathbf{r}_i} - \frac{\partial E^{\text{q-p}}}{\partial \mathbf{r}_i} - \frac{\partial E^{\text{p-p}}}{\partial \mathbf{r}_i}$$

$$\sum_{j=1;i\neq j}^{N} \mathrm{T}_{ij}^{q-q} q_j - \sum_{j=1;i\neq j}^{N} \mathrm{T}_{ij}^{q-p} \mathbf{p}_j + T_{ii}^{q-q} q_i + T_{ii}^{q-p} \mathbf{p}_i = -\chi_i$$

$$\sum_{j=1;i\neq j}^{N} \mathrm{T}_{ij}^{q-p} q_j + \sum_{j=1;i\neq j}^{N} \mathrm{T}_{ij}^{p-p} \mathbf{p}_j + T_{ii}^{q-p} q_i + T_{ii}^{p-p} \mathbf{p}_i = 0$$

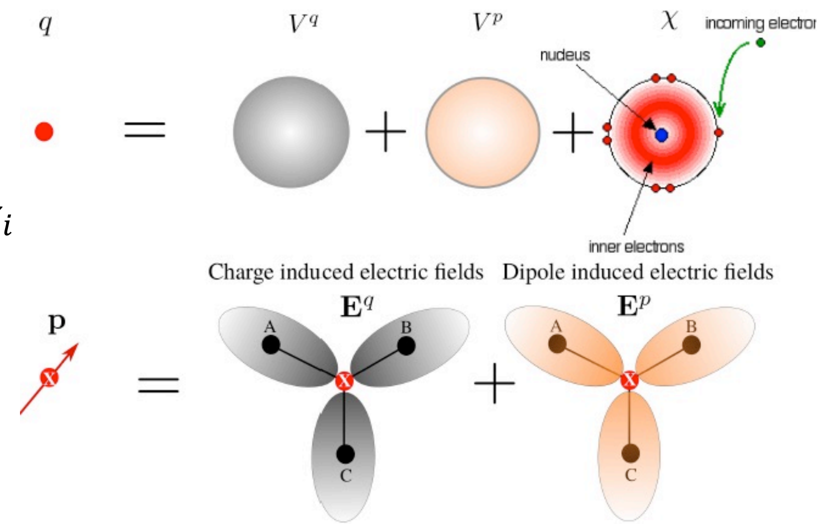

Initial cords + potential parameters → Loading conditions + Evaluating CD forces → Extracting q, p, electric fields, voltages etc → Calculating coefficients from the polarization response

Highly beneficial over DFT, wide scope for investigating large deformations

Nanotechnology 29 (22), 225702 (2018); Phys. Rev. B, 99, 054105 (2019)

Flexoelectric coefficient of graphene
Charge dipole model

$$P^z = \mu^{zzxx} K_{out}$$

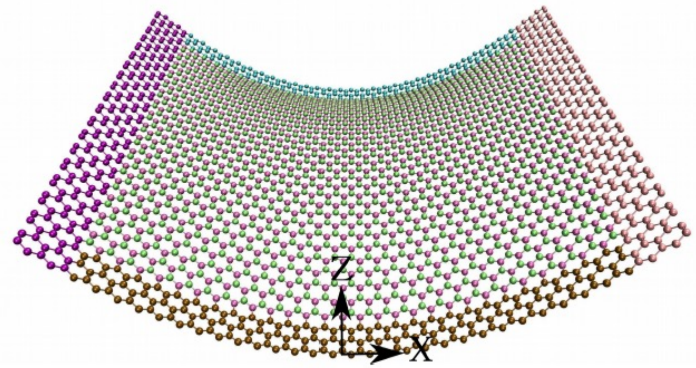

out-plane bending

$$P^y = \mu^{yyxx} K_{in}$$

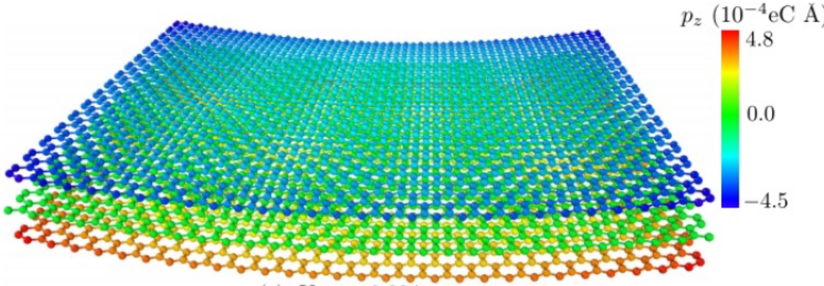

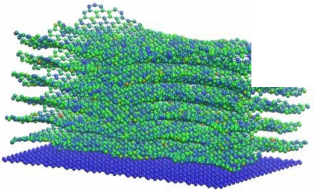

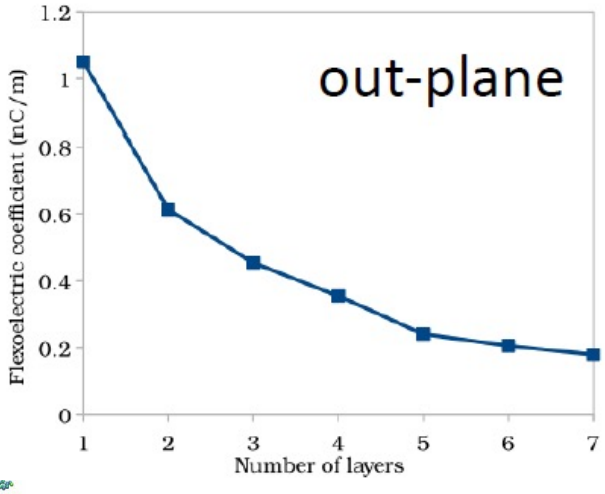

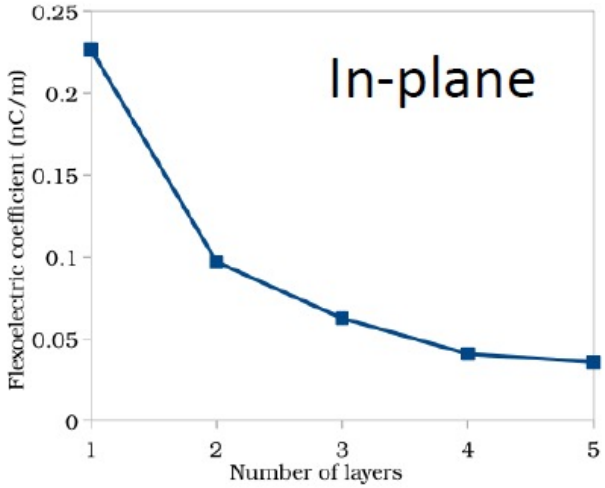

Flexoelectric coefficient of graphene

Charge dipole model

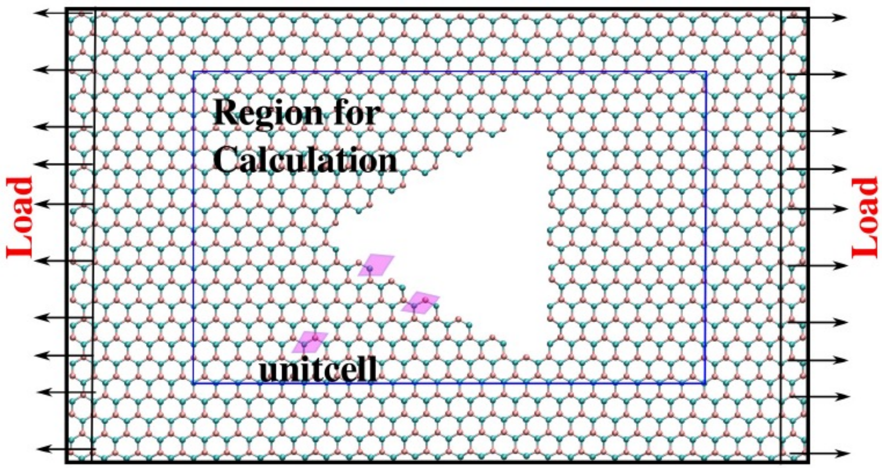

Schematic atomic configuration with loading conditions

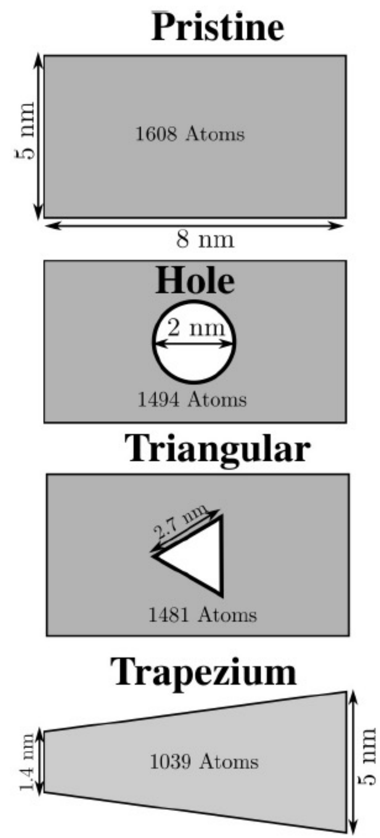

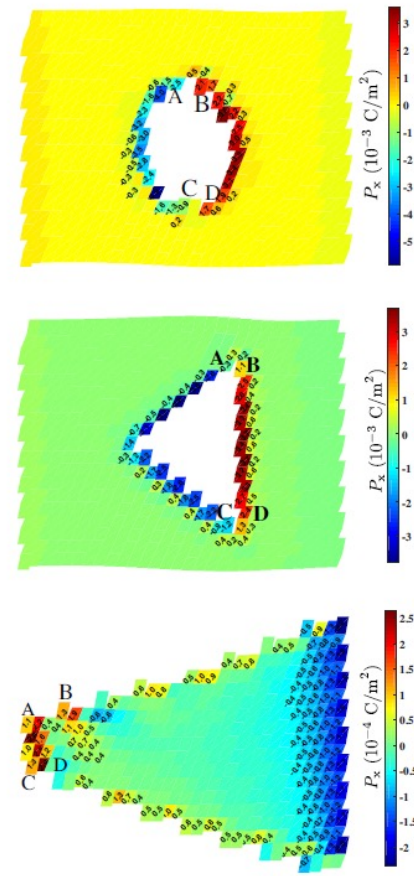

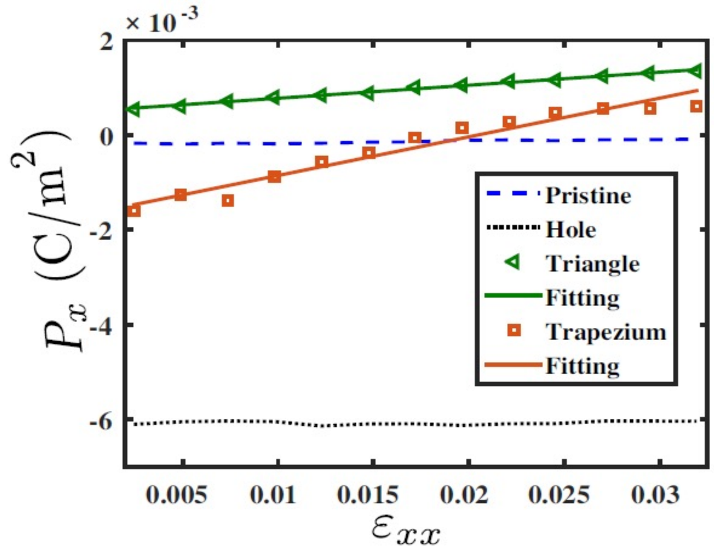

Graphene with triangular defect

$d_{xxx} = 0.02826\ \mathrm{C/m^2}$

$\mathbf{P}_x^{\mathrm{f}} = 5.01152 \times 10^{-4}\ \mathrm{C/m^2}$

$d_{xxx} = 0.08013\ \mathrm{C/m^2}$

$\mathbf{P}_x^{\mathrm{f}} = -16.67440 \times 10^{-4}\ \mathrm{C/m^2}$

B. Javvaji, B. He and X. Zhuang. The generation of piezoelectricity and flexoelectricity in graphene by breaking the materials symmetries. Nanotechnology, 29: 225702 , 2018.

Flexoelectric coefficient of graphene

Bending induced out of plane polarization

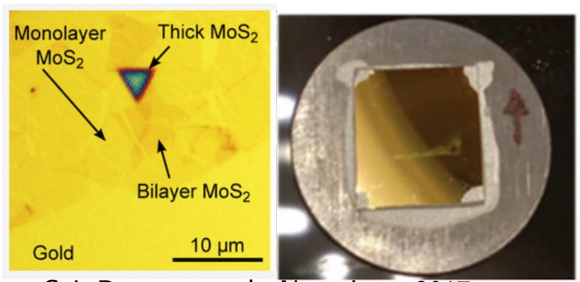

C.J. Brennan et al., Nano Lett. 2017

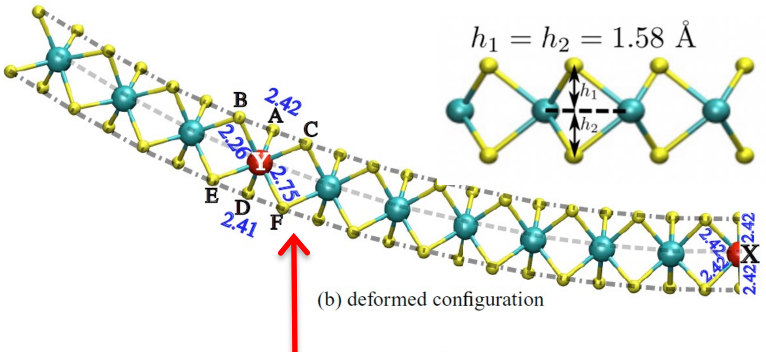

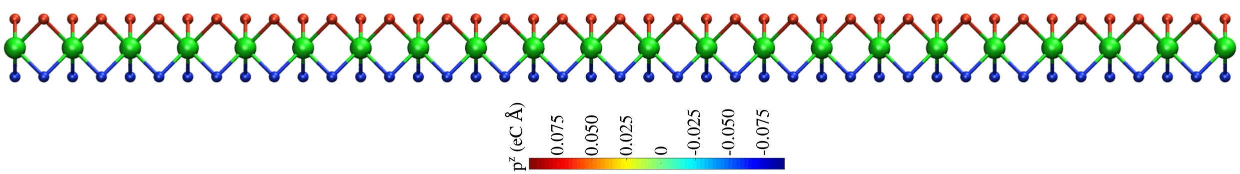

X. Zhuang, B. He, B. Javvaji, H.S. Park. Intrinsic bending flexoelectric constants in two-dimensional materials, Physical Review B, 2019

MoS2 response with MTP model

Response of MoS2 monolayer with SW potential and MTP potential

No change in CD parameters

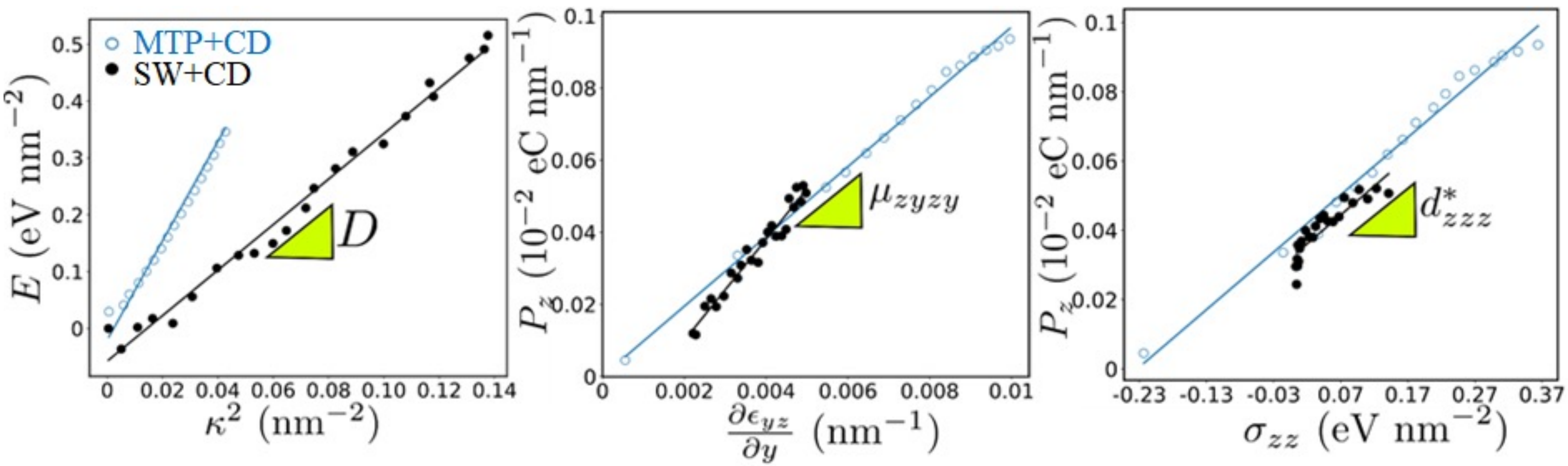

The polarization response with strain gradient and with stress is highly linear

Response with MTP

	MTP+CD	SW+CD	Experimental results
μ (nC/m)	**0.023**	0.025 (poor linear fitting issues)	0.091 (C.J. Brennan et al., Nano Lett. 2017)
d_{33}^{*} (pm/V)	**1.64**	1.681 (poor linear fitting)	1-1.5 (C.J. Brennan et al., Nano Lett. 2017)
D (eV)	**16.51**	8.314	9 to 16 eV (several reports)
E (N/m)	**135**	100	130 to 180 (several reports)

The results from MTP+CD model compare well with the experiments.

Flexoelectricity in graphene crumpling

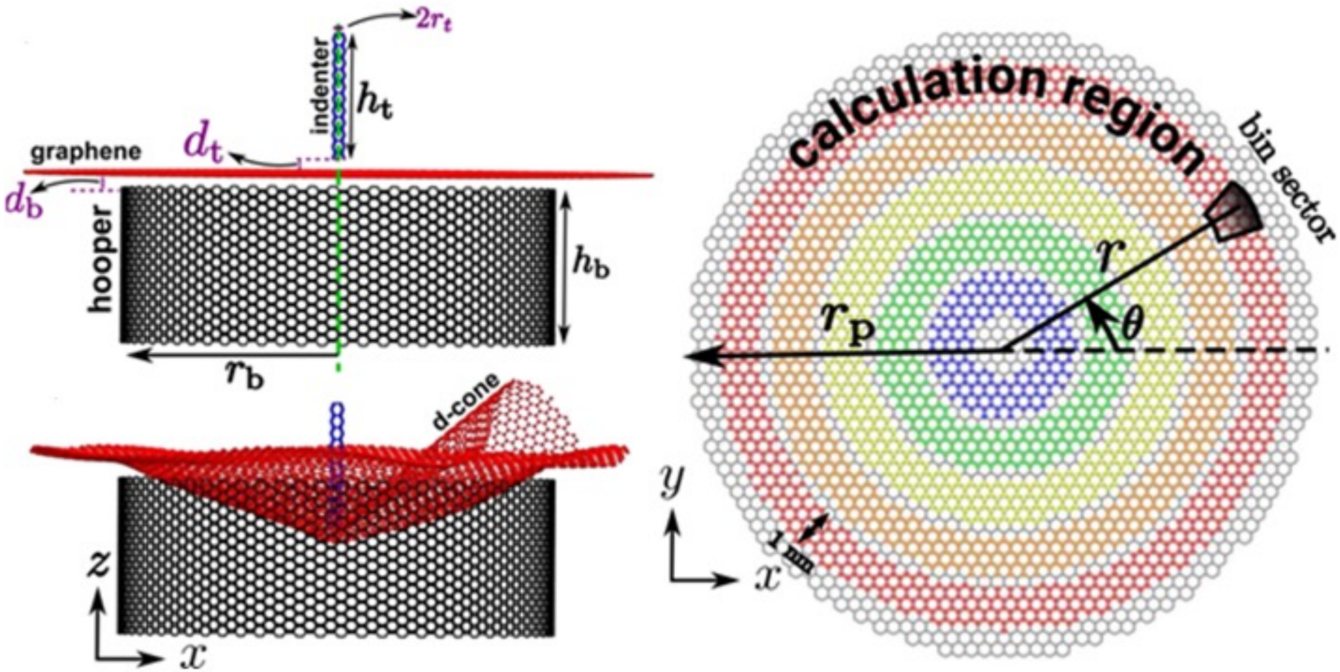

- Consider circular graphene nanoribbon as an example
- Hooper CNT held fixed and indenter moves with constant speed
- No other conditions are imposed
- Curvature variation confirms the d-cone structure due to crumpling

Graphene crumpling response

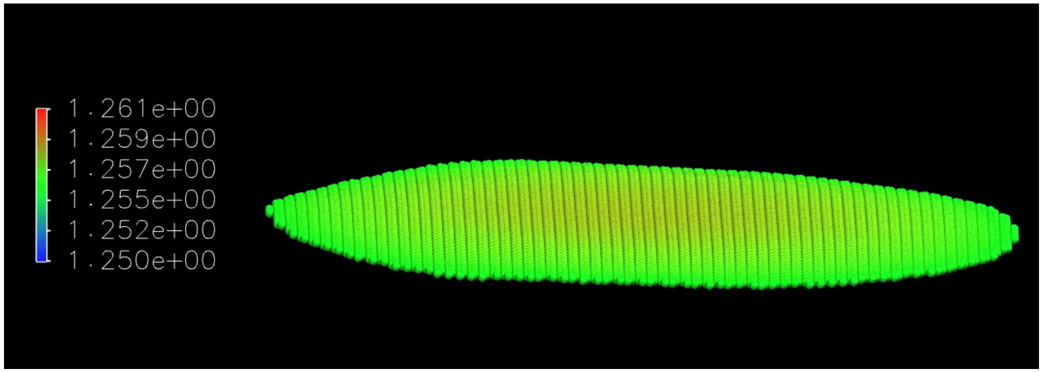

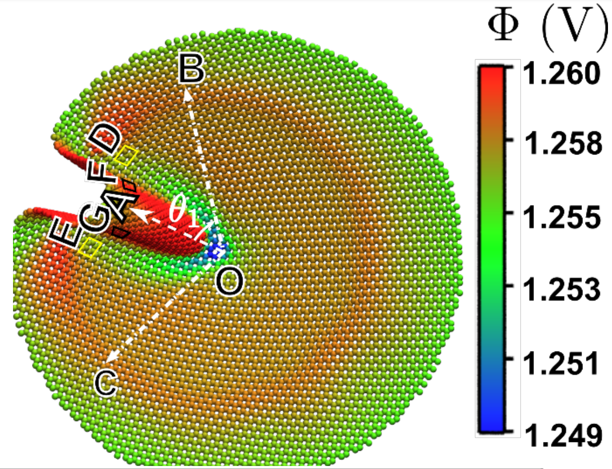

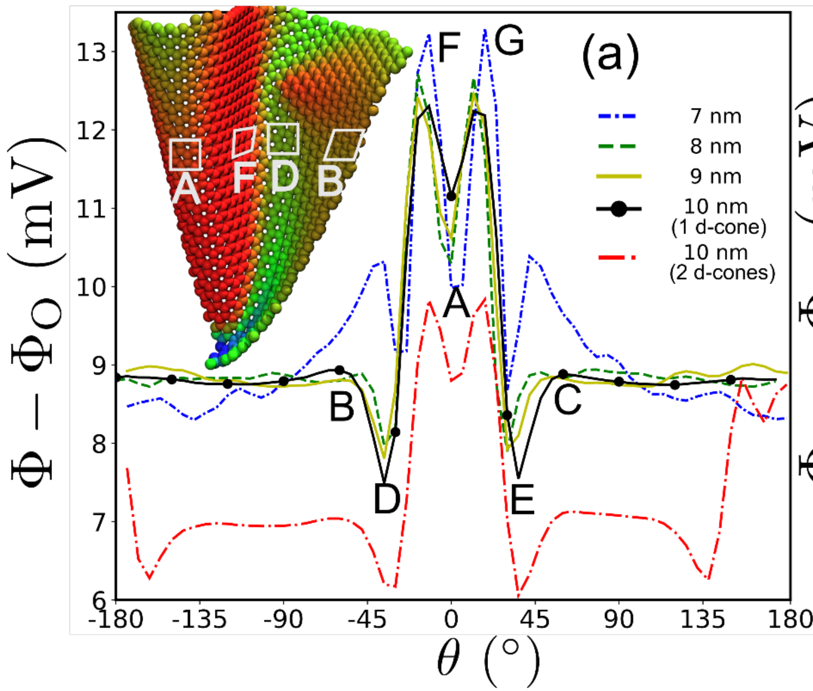

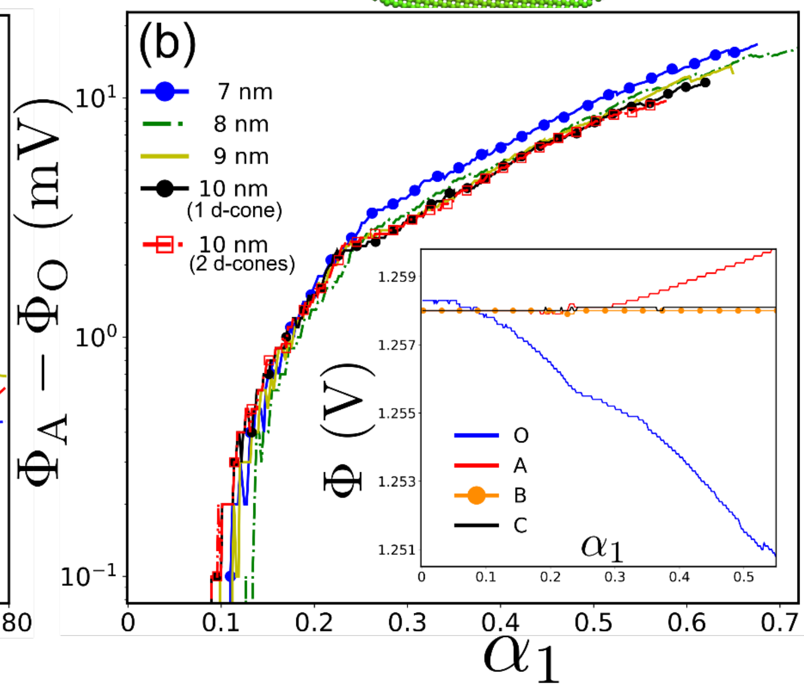

Javvaji, Zhang, Park, Zhuang., J. Appl. Phys., 2021, 129, 225107

Overview

- Atomic-scale model of flexoelectric materials
- Nano-continuum scale model of flexoelectric structures
- Microscale model of flexoelectric composites
- Macroscale application with phonic topological insulator

Model for flexoelectricity

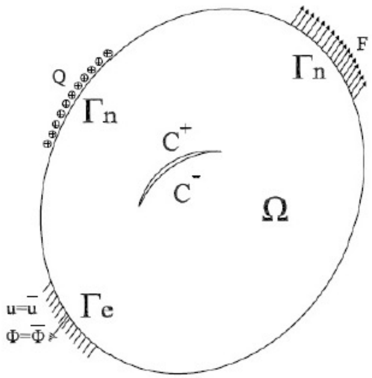

Balance equations of electric and mechanical fields

$$\nabla \cdot \sigma + b = 0 \qquad \text{in } \boldsymbol{\Omega}$$

$$\nabla \cdot \mathbf{D} - q = 0 \qquad \text{in } \boldsymbol{\Omega}$$

$$\nabla_s \cdot \sigma_s = 0 \qquad \text{on } \boldsymbol{\Gamma}$$

$$\nabla_s \cdot D_s = 0 \qquad \text{on } \boldsymbol{\Gamma}$$

Energy density function of flexoelectric materials

flexoelectric related terms

$$U = U_b + U_s$$

$$U_b = \frac{1}{2}\boldsymbol{\epsilon} : \mathbf{C} : \boldsymbol{\epsilon} - \mathbf{E} \cdot \mathbf{e} : \boldsymbol{\epsilon} - \boxed{\mathbf{E} \cdot \mathrm{h} \vdots \boldsymbol{\eta}} - \frac{1}{2}\boldsymbol{E} \cdot \boldsymbol{\kappa} \cdot \boldsymbol{E} + \boxed{\frac{1}{2}\boldsymbol{\eta} \vdots \boldsymbol{g} \vdots \boldsymbol{\eta}}$$

$$U_s = U_{s0} + \boldsymbol{\alpha_s} : \boldsymbol{\epsilon_s} + \boldsymbol{\omega_s} \cdot \mathbf{E}_\mathrm{s} + \frac{1}{2}\boldsymbol{\epsilon_s} : \mathbf{C}_s : \boldsymbol{\epsilon_s} - \mathbf{E}_\mathrm{s} \cdot \mathbf{e}_\mathrm{s} : \boldsymbol{\epsilon_s} - \frac{1}{2}\boldsymbol{E_s} \cdot \boldsymbol{\kappa_s} \cdot \boldsymbol{E_s}$$

g: the sixth order tensor of strain gradient elasticity

$h =$ d-f is the outcome of converse-flexoelectricity and flexoelectricity

η is the strain gradient tensor

S.S. Nanthakumar, X. Zhuang, H.S. Park, T. Rabczuk. Topology optimization of flexoelectric nano energy harvester. Journal of the Mechanics and Physics of Solids, 105:217-234, 2017.

Model for flexoelectricity

CSST Chair of Computational Science and Simulation Technology

Constitutive equations

$$\boldsymbol{\sigma}^b = \boldsymbol{\sigma} - \nabla \cdot \boldsymbol{\tau} = \frac{\partial U_b}{\partial \epsilon} - \nabla \cdot \left(\frac{\partial U_b}{\partial \eta} \right) = C : \epsilon - E \cdot e + \boxed{\nabla E : h}$$

$$D^b = -D - \nabla \cdot Q = -\frac{\partial U_b}{\partial E} - \nabla \cdot \left(\frac{\partial U_b}{\partial \nabla E} \right) = e \cdot \epsilon + \kappa \cdot E + \boxed{h \vdots \eta}$$

$$\boldsymbol{\sigma_s} = \boldsymbol{\tau_s} + \mathbb{C}_s : \boldsymbol{\epsilon}_s - \boldsymbol{e_s} \cdot \boldsymbol{E_s}$$

$$\boldsymbol{D_s} = \boldsymbol{\omega_s} + \boldsymbol{e_s}^T : \boldsymbol{\epsilon_s} + \boldsymbol{\kappa}_s \cdot \boldsymbol{E}_s$$

C and C_s	fourth-order elastic bulk and surface stiffness tensors
e and e_s	bulk and surface piezoelectric third order tensors,
τ_s and ω_s	residual surface stress and electric field.
ε and E	bulk strain tensor and bulk electric field vector
ε_s and E_s	corresponding surface counterparts.

Higher order continuity

Commercial FE software however provides only C0 continuity

C^1 continuity

$$U = U_b + U_s$$

$$U_b = \frac{1}{2}\epsilon : \mathbf{C} : \epsilon - \mathbf{E}\cdot\mathbf{e} : \epsilon - \boxed{\mathbf{E}\cdot\mathbf{h}\,\vdots\,\boldsymbol{\eta}} - \frac{1}{2}\boldsymbol{E}\cdot\boldsymbol{\kappa}\cdot\boldsymbol{E} + \boxed{\frac{1}{2}\boldsymbol{\eta}\,\vdots\,\boldsymbol{g}\,\vdots\,\boldsymbol{\eta}}$$

$$U_s = U_{s0} + \boldsymbol{\alpha_s} : \boldsymbol{\epsilon_s} + \boldsymbol{\omega_s}\cdot\mathbf{E}_s + \frac{1}{2}\boldsymbol{\epsilon_s} : \mathbf{C}_s : \boldsymbol{\epsilon_s} - \mathbf{E}_s\cdot\mathbf{e}_s : \boldsymbol{\epsilon_s} - \frac{1}{2}\boldsymbol{E_s}\cdot\boldsymbol{\kappa_s}\cdot\boldsymbol{E_s}$$

IGA (IsoGeometric Analysis)
Based on non-uniform B-Splines

$$u_h(x,y) = \sum_{i=1}^{ncp}\sum_{j=1}^{mcp} N_{i,j}^{p,q}(\xi,\eta)\,u_{ij}^e = (\boldsymbol{N}_u)^{\mathrm{T}}\boldsymbol{u}^e$$

$$\theta_h(x,y) = \sum_{i=1}^{ncp}\sum_{j=1}^{mcp} N_{i,j}^{p,q}(\xi,\eta)\,\theta_{ij}^e = (\boldsymbol{N}_\theta)^{\mathrm{T}}\boldsymbol{\theta}^e$$

Alternatively, one can use meshless methods

CaInterfaces by jump enrichment

CSST
Chair of Computational Science and Simulation Technology

The displacement field, $\boldsymbol{u^h}$ and electric potential field, $\boldsymbol{\phi^h}$ for a piezoelectric material in the XFEM formulation are expressed as:

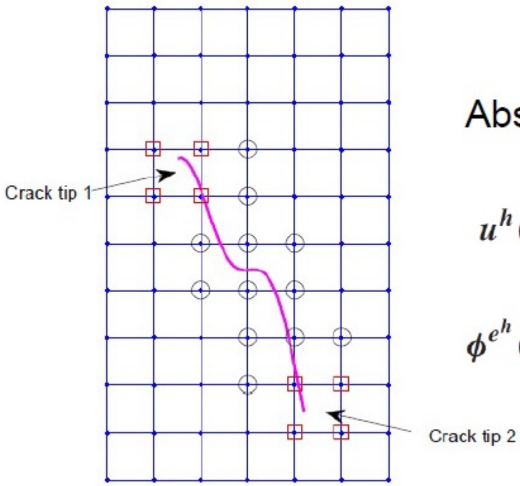

Abs enrichment

$$\boldsymbol{u}^h(\mathrm{X}) = \sum_{i\in I} N_i(\mathrm{X})\boldsymbol{u}_i + \sum_{N=1}^{n_c}\sum_{l\in L} N_l(\mathrm{X})\boldsymbol{a}_l^{(N)} f_l^{(N)}$$

$$\boldsymbol{\phi}^{e^h}(\mathrm{X}) = \sum_{i\in I} N_i(\mathrm{X})\boldsymbol{\phi}_i^e + \sum_{N=1}^{n_c}\sum_{l\in L} N_l(\mathrm{X})\boldsymbol{\alpha}_l^{(N)} f_l^{(N)}$$

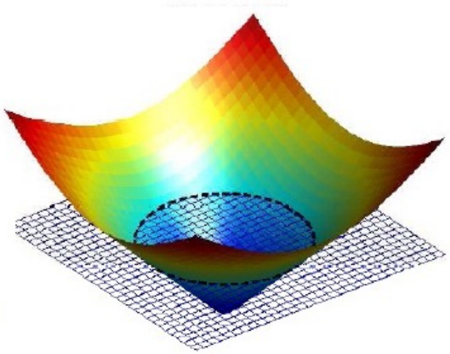

$$u^h(x) = \sum_{i\in I} N_i(X)u_i + \sum_{N=1}^{n_c}\sum_{j\in J} N_j(X)a_j^{(N)}\psi_I^{(N)} + \sum_{M=1}^{m_t}\sum_{k\in K} N_k(X)\left(\sum_{i=1}^{4}\Phi_i{}^{(M)}(r,\theta)b_k^i\right)$$

$$\phi^h(x) = \sum_{i\in I} N_i(X)\phi_i + \sum_{N=1}^{n_c}\sum_{j\in J} N_j(X)\alpha_j^{(N)}\psi_I^{(N)} + \sum_{M=1}^{m_t}\sum_{k\in K} N_k(X)\left(\sum_{i=1}^{4}\Phi_i{}^{(M)}(r,\theta)\beta_k^i\right)$$

$$\left[\boldsymbol{K}^{UU}\right]\begin{Bmatrix} u \\ a \end{Bmatrix} + \left[\boldsymbol{K}^{U\Phi}\right]\begin{Bmatrix} \phi^e \\ \alpha \end{Bmatrix} = \begin{Bmatrix} f_u \\ f_u^a \end{Bmatrix}$$

$$\left[\boldsymbol{K}^{\Phi U}\right]\begin{Bmatrix} u \\ a \end{Bmatrix} - \left[\boldsymbol{K}^{\Phi\Phi}\right]\begin{Bmatrix} \phi^e \\ \alpha \end{Bmatrix} = \begin{Bmatrix} f_\phi \\ f_\phi^\alpha \end{Bmatrix}$$

Discrete equations for coupling between stress and polarization

Optimization using the level sets

- Shape deriv. and level sets to find geometry with min. compliance
- Shape deriv. as normal velocity of free boundary
- Front propagation by solution of Hamilton-Jacobi equation for a level set function
- Shape is capture on a fixed Eulerian mesh.

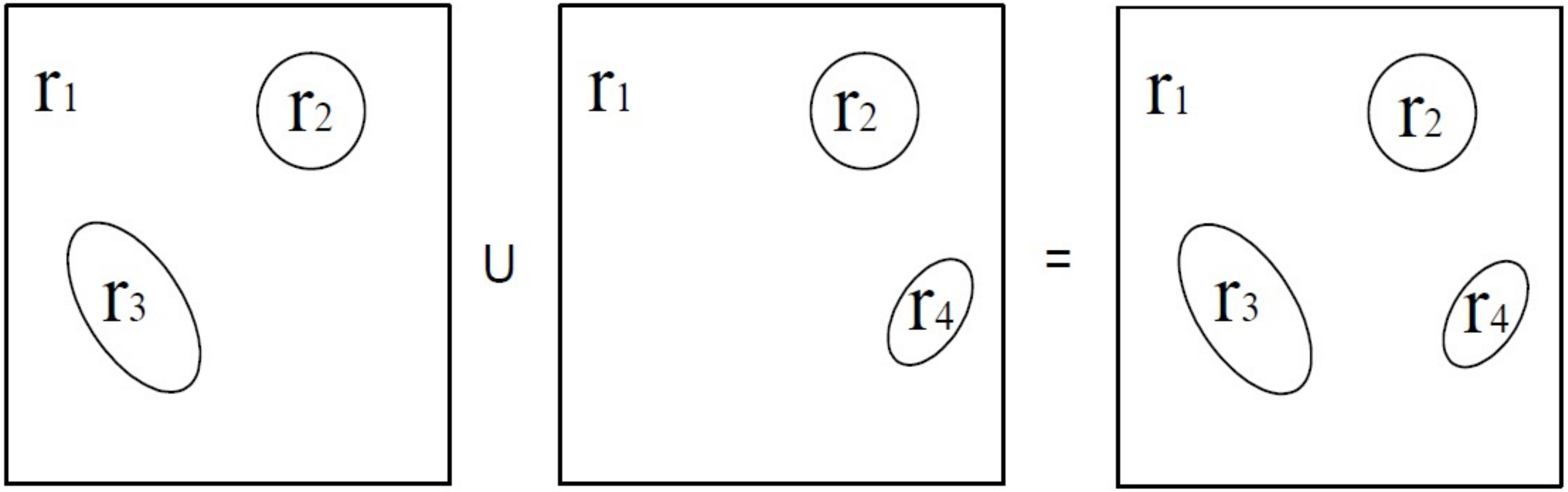

Figure: Multiple level sets representation : The union of two level set functions, $\phi1$ and $\phi2$ gives the actual domain with inclusions.

Topology representation with level sets

Single level set

$$r = \frac{1}{2}[r_1(1 + sign(\Phi)) + r_2(1 - sign(\Phi))].$$

Multiple level sets

$$r = \frac{1}{4}[r_1(1+S_1)(1+S_2) + r_2(1-S_1)(1-S_2) + r_3(1-S_1)(1+S_2) + r_4(1+S_1)(1-S_2)]$$

S_1 and S_2 corresspond to the sign of the level set functions ϕ_1 and ϕ_2 respectively. r_1, r_2, r_3 and r_4 are material ratios in the four regions.

Robustness of level sets in modelling

The level set method is suitable for highly evolving geometry

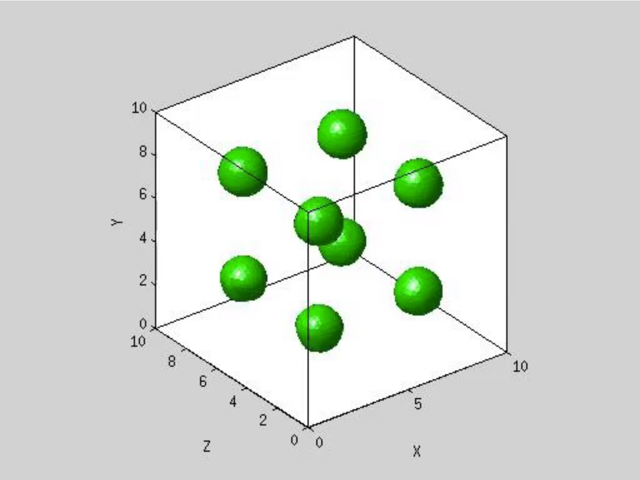

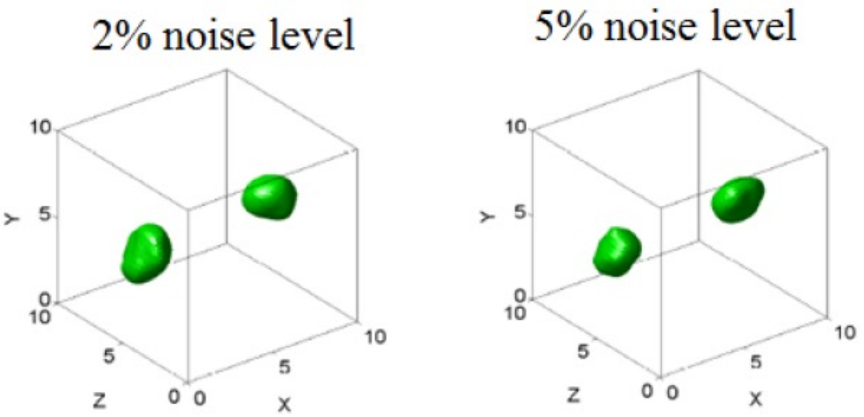

Convergence to objective func.

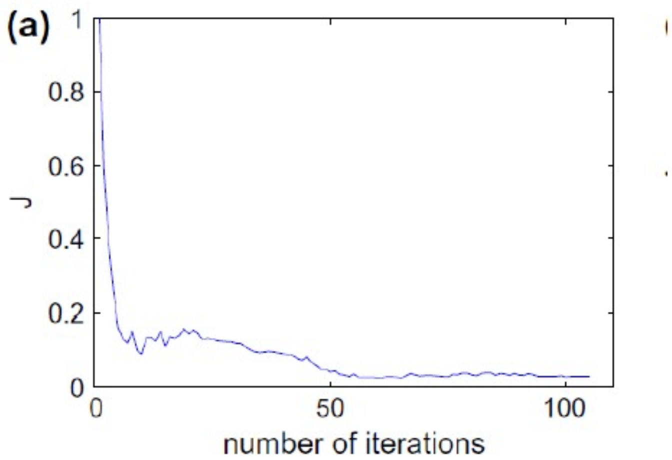

L- curve for stability

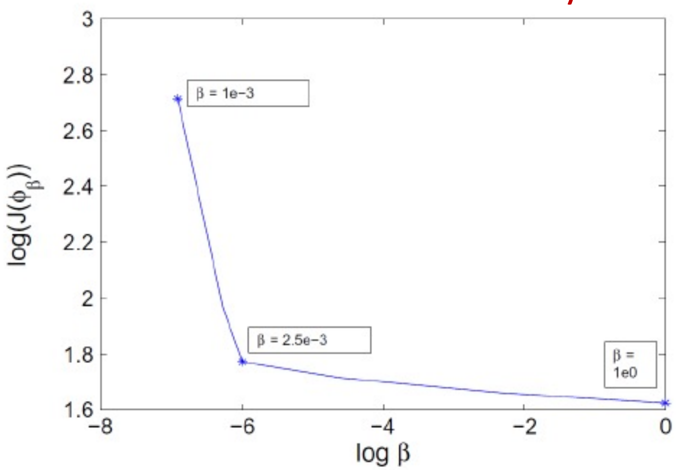

Electromechanical coupling coefficient

$$k^2 = \frac{\Pi_e}{\Pi_m}$$

$$\Pi_e = \frac{1}{2}\int_\Omega \boldsymbol{E}(\phi)^T \boldsymbol{\kappa} \boldsymbol{E}(\phi) d\Omega + \frac{1}{2}\int_\Gamma \boldsymbol{E^s}(\phi)^T \boldsymbol{\kappa^s} \boldsymbol{E^s}(\phi) d\Gamma = \frac{1}{2}\phi^{\boldsymbol{T}}(\boldsymbol{K}_{\boldsymbol{\phi\phi}} + \boldsymbol{K}^s_{\boldsymbol{\phi\phi}})\phi$$

$$\Pi_m = \frac{1}{2}\int_\Omega \boldsymbol{\epsilon}(\boldsymbol{u})^T \boldsymbol{C} \boldsymbol{\epsilon}(\boldsymbol{u}) d\Omega + \frac{1}{2}\int_\Gamma \boldsymbol{\epsilon^s}(\boldsymbol{u})^T \boldsymbol{C^s} \boldsymbol{\epsilon^s}(\boldsymbol{u}) d\Gamma = \frac{1}{2}\boldsymbol{u}^{\boldsymbol{T}}(\boldsymbol{K}_{\boldsymbol{uu}} + \boldsymbol{K}^{\boldsymbol{s}}_{\boldsymbol{uu}})\boldsymbol{u}$$

Objective function and constraints

$$\boxed{\text{Minimize} \quad J(\Psi) = \frac{1}{k^2} = \frac{\Pi_m}{\Pi_e}}$$

$$\text{Subject to} \quad \int_\Omega d\Omega - \bar{V} = 0$$

$$\text{and} \quad \delta\Pi = 0$$

Surface effects plays the role over sizes

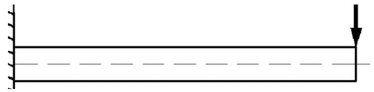

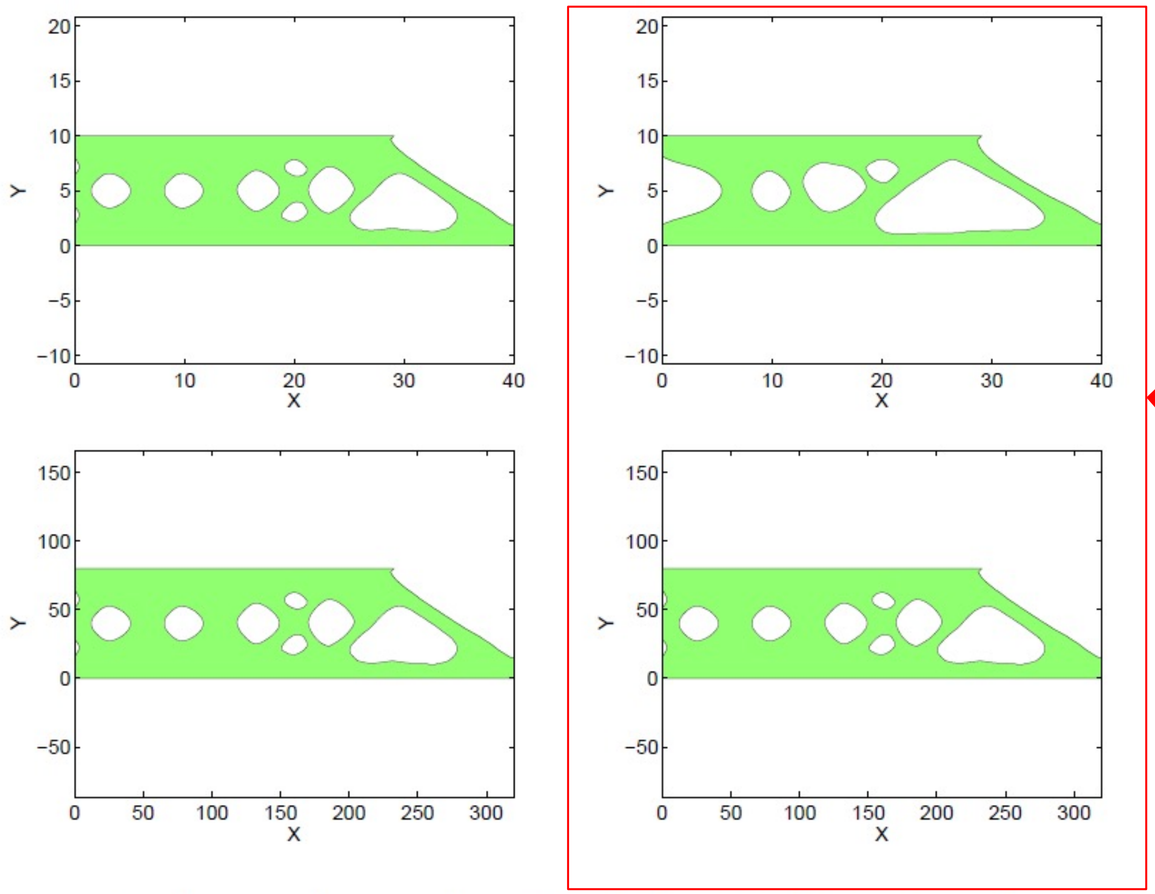

With surface effects

Figure: The optimal topology obtained for J objective function for 40x10 nm and 320x80 nm cantilever beams without surface effects left and with surface effects right.

Surface effects plays the role over sizes

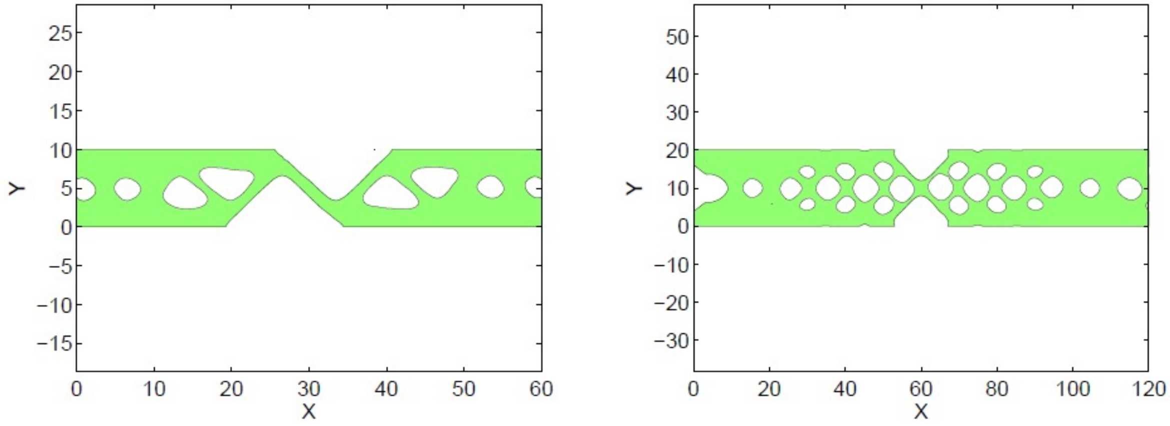

Figure: Optimal topology for objective function J for (a) 60x10 nm and (b) 120x20 nm fixed nanobeam.

Influence of boundary conditions and size effects

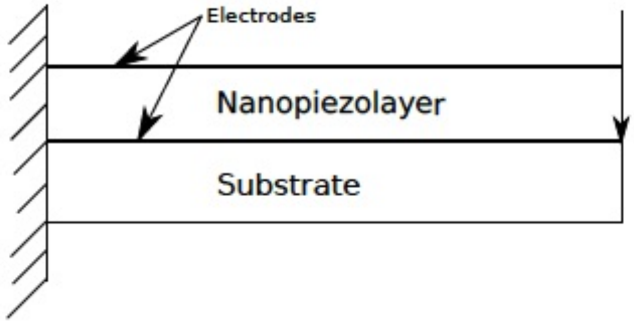

boundary conditions and sizes effects are most dominant factors

Open circuit

size	nominal EMCC ($C^s \neq 0, e^s \neq 0$)
Aspect ratio = 4	
40×10	1.19
80×20	1.13
160×40	1.1
Aspect ratio = 8	
80×10	1.15
160×20	1.095
240×30	1.06

Closed circuit

size	nominal EMCC ($C^s \neq 0, e^s \neq 0$)
Aspect ratio = 4	
40×10	2.5
80×20	2.2
160×40	2.1
Aspect ratio = 8	
80×10	2.6
160×20	2.3
240×30	2.2

S.S. Nanthakumar, T. Lahmer, X. Zhuang, H.S. Park, T. Rabczuk. Topology Optimization of Piezoelectric Nanostructures, Journal of the Mechanics and Physics of Solids, 94:316-335, 2016.

Influence of the boundary conditions

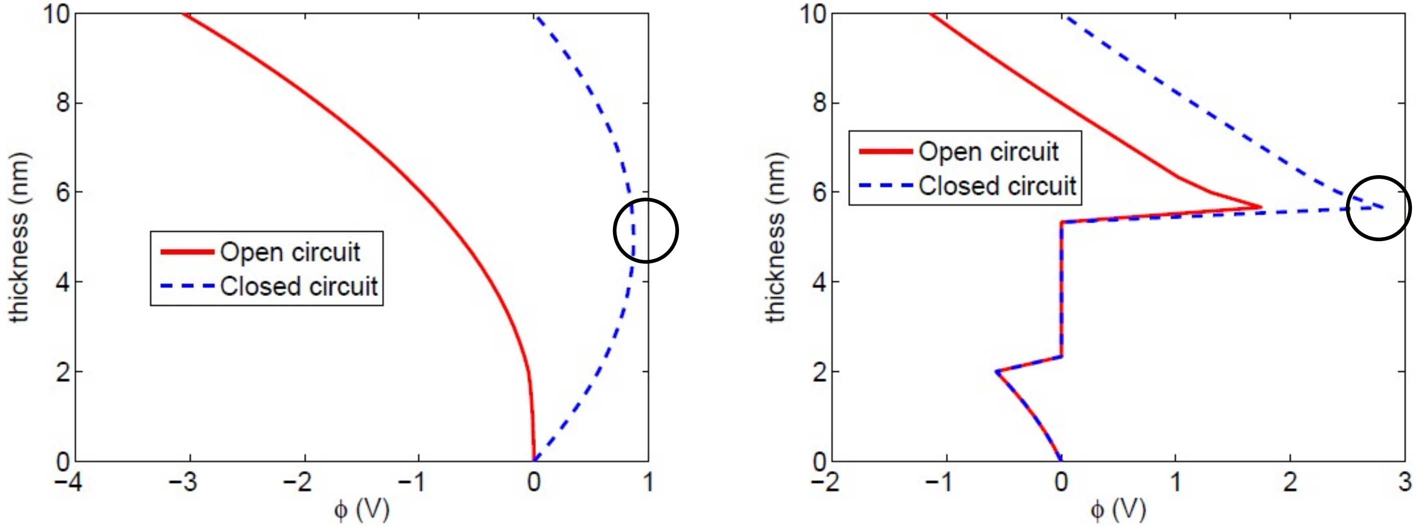

Figure: Electric potential distribution across the thickness of the 40 $\times$ 10 nm, (a) Solid beam (b) Optimal beam, at $x = 10$ nm.

S.S. Nanthakumar, T. Lahmer, X. Zhuang, H.S. Park, T. Rabczuk. Topology Optimization of Piezoelectric Nanostructures, Journal of the Mechanics and Physics of Solids, 94:316-335, 2016.

Interplay of surface piezo and surface elasticity

CSST Chair of Computational Science and Simulation Technology

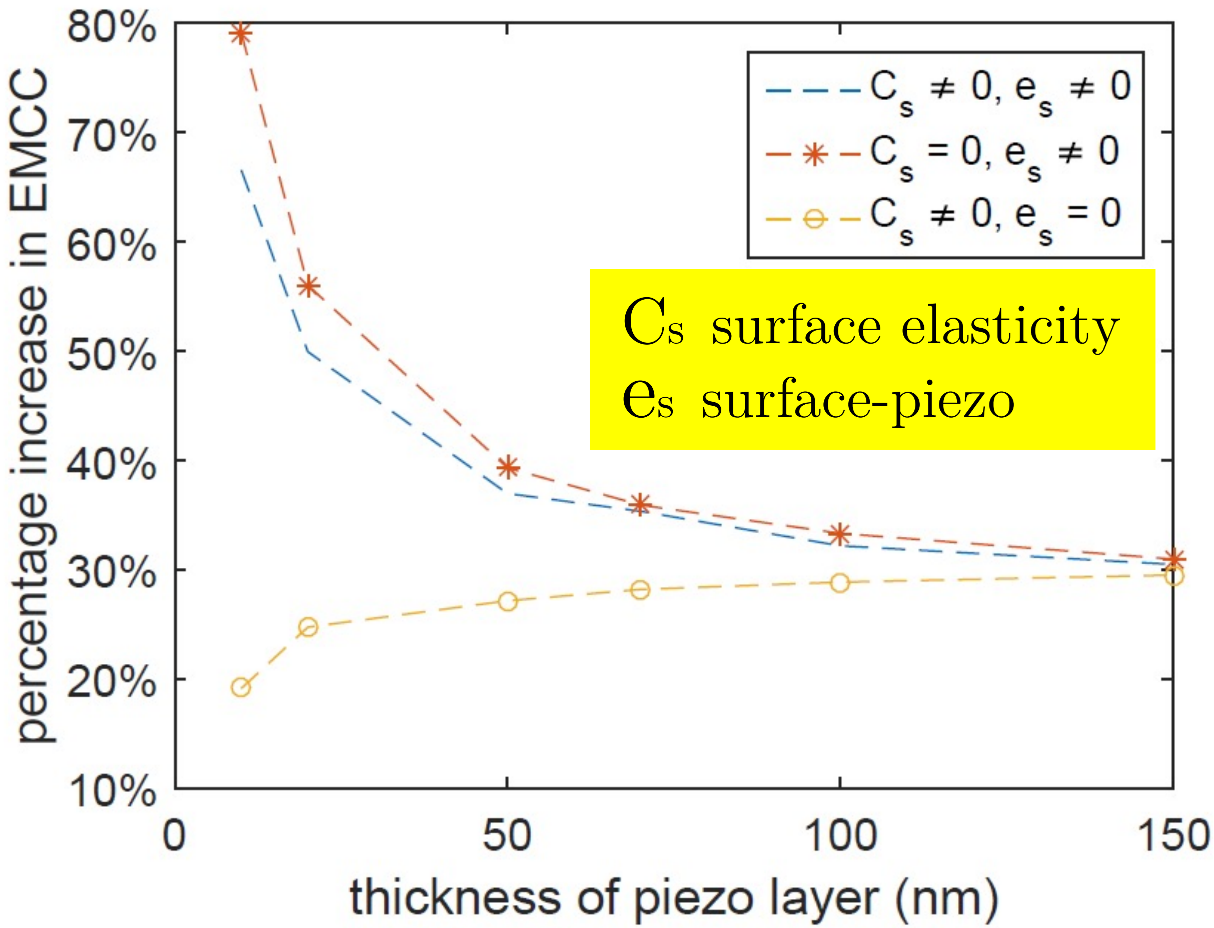

C_s surface elasticity

e_s surface-piezo

BTO plate topology optimization wrt ECC

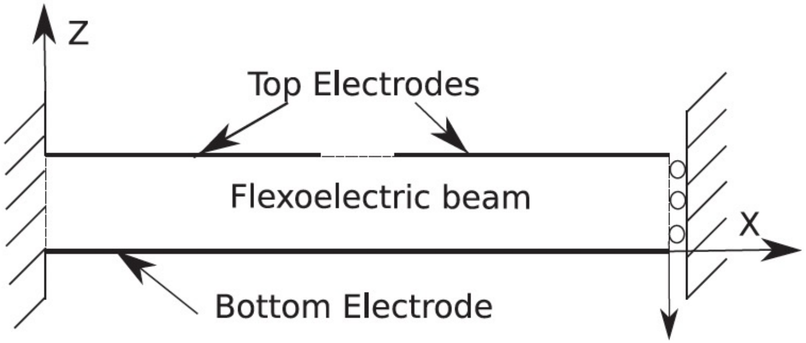

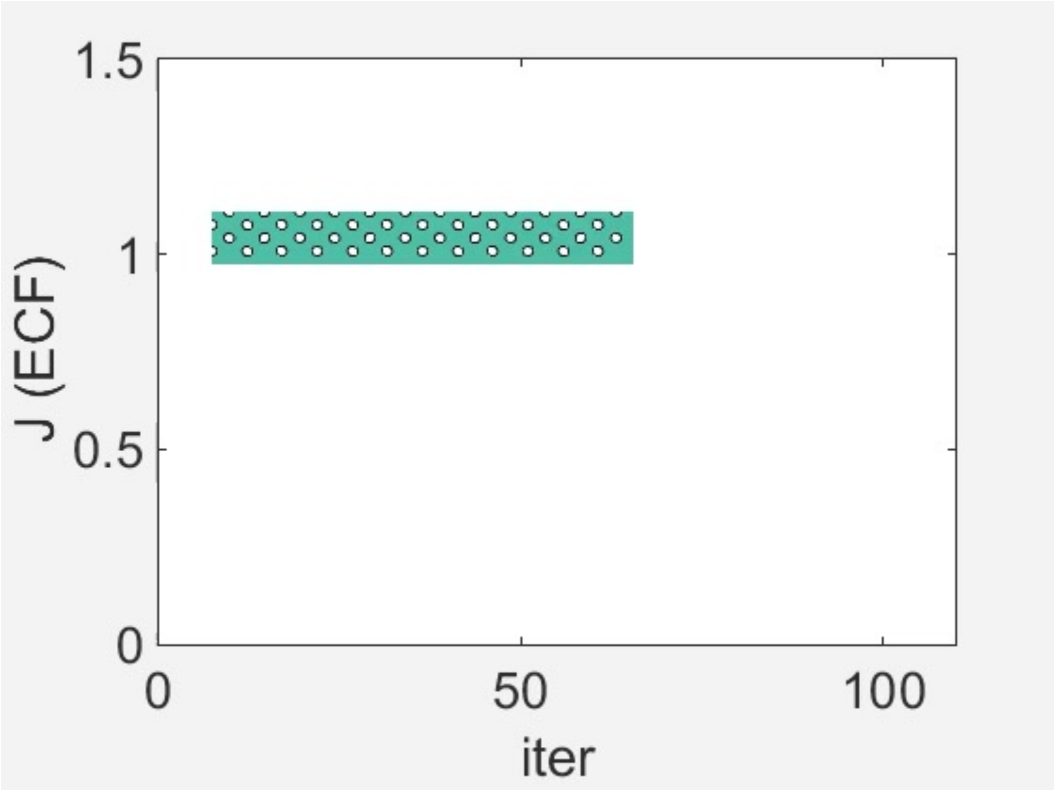

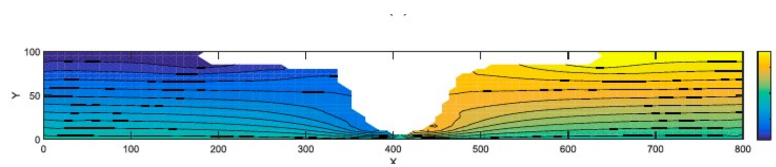

Test examples

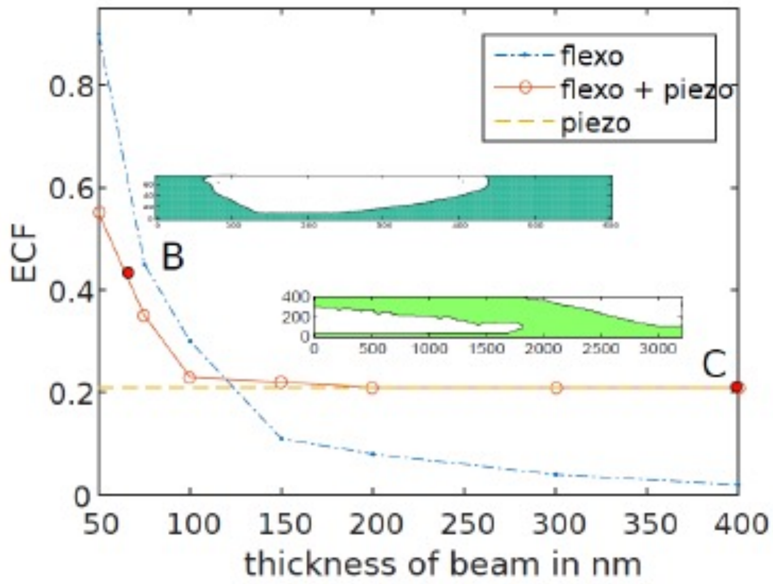

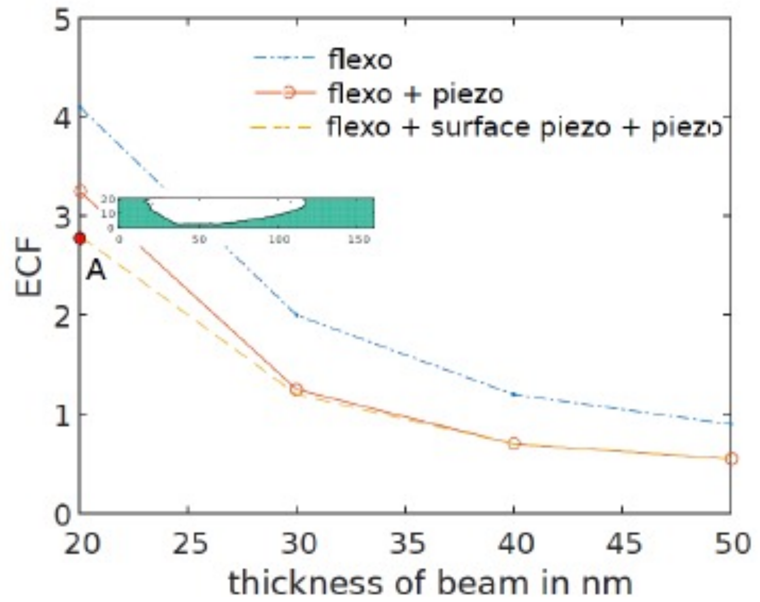

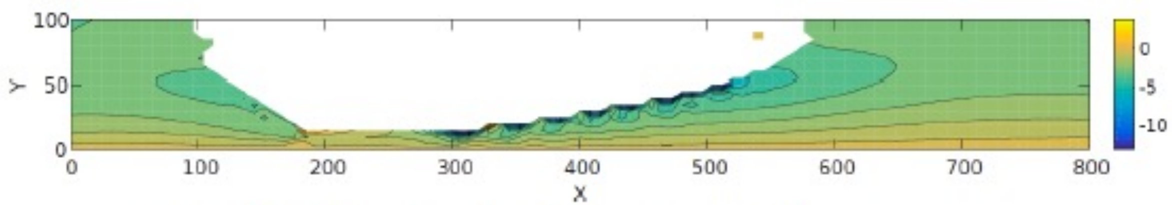

Distribution of electric potential

S.S. Nanthakumar, X. Zhuang, H.S. Park, T. Rabczuk. Topology optimization of flexoelectric nano energy harvester. Journal of the Mechanics and Physics of Solids, 105:217-234, 2017.

Plate energy harvester

$$\nabla \cdot \boldsymbol{\sigma} + \boldsymbol{b} = 0 \qquad \text{in } \boldsymbol{\Omega}$$
$$\nabla \cdot \mathrm{D} - q = 0 \qquad \text{in } \boldsymbol{\Omega}$$
$$\nabla_s \cdot \boldsymbol{\sigma}_s = 0 \qquad \text{on } \boldsymbol{\Gamma}$$
$$\nabla_s \cdot \boldsymbol{D}_s = 0 \qquad \text{on } \boldsymbol{\Gamma}$$

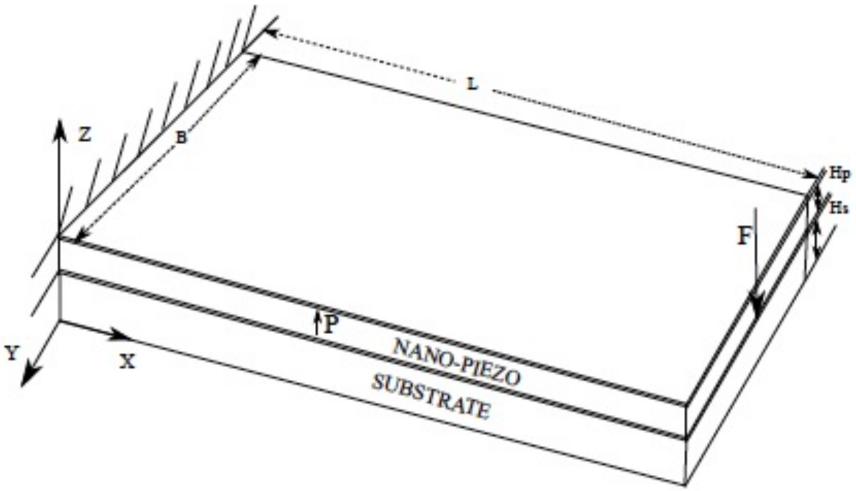

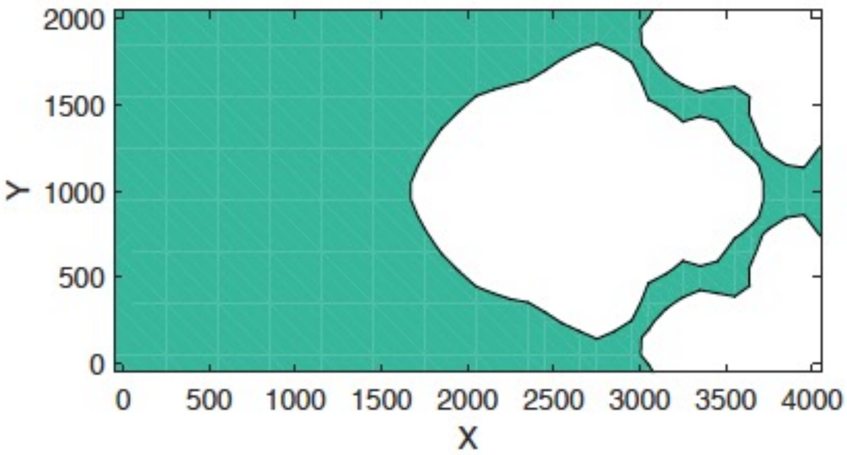

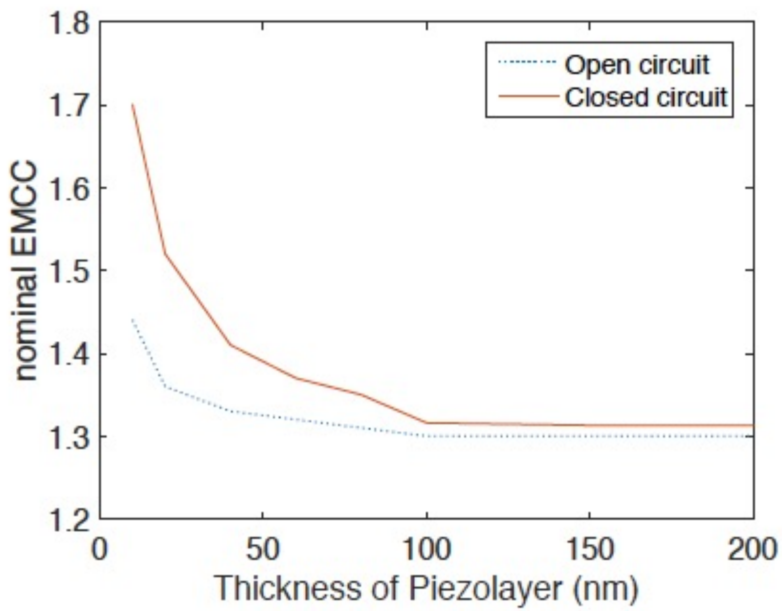

Design of flexoelectric energy harvester

CSST
Chair of Computational Science and Simulation Technology

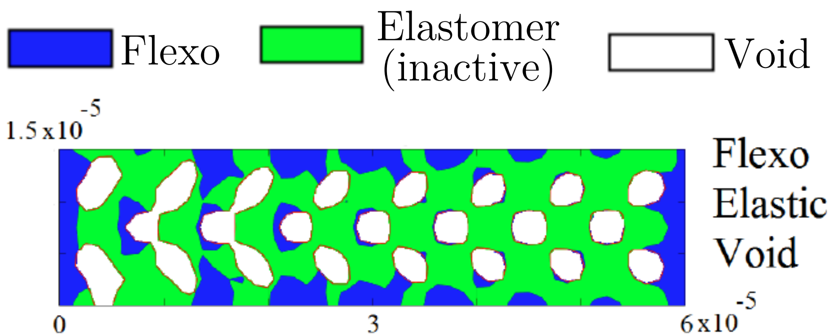

Flexo 28%
Elastic 42%
Void 30%

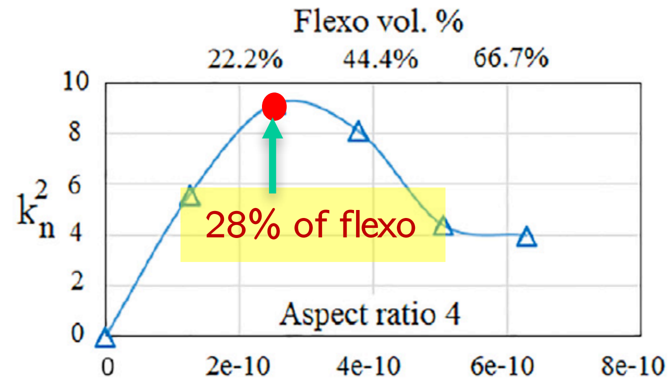

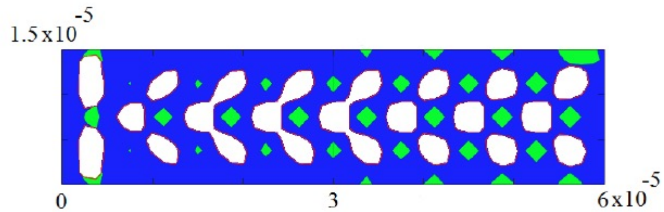

Flexo 56%
Elastic 14%
Void 30%

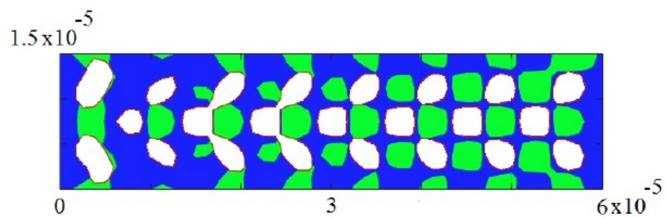

Flexo 42%
Elastic 28%
Void 30%

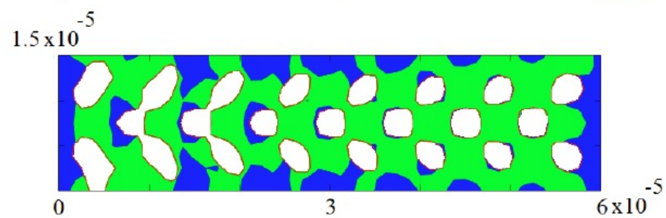

Flexo 28%
Elastic 42%
Void 30%

IGA (IsoGeometric Analysis)
Based on non-uniform B-Splines

Topology Optimization of flexoelectric structures, Journal of the Mechanics and Physics of Solids, 105:217-234, 2017.
Sensitivity and uncertainty analyses for flexoelectric nanostructures. Computer Methods in Applied Mechanics and Engineering, 337:95-109, 2018.

Overview

- Atomic-scale model of flexoelectric materials
- Nano-continuum scale model of flexoelectric structures
- Microscale model of flexoelectric composites
- Macroscale application with phonic topological insulator

Non-trivial bandgap

- For low-frequency surface wave manipulation, we design a honeycomb lattice of pillars on the surface of elastic medium.
- Induced non-trivial bandgap can **provide robust surface wave attenuation**.

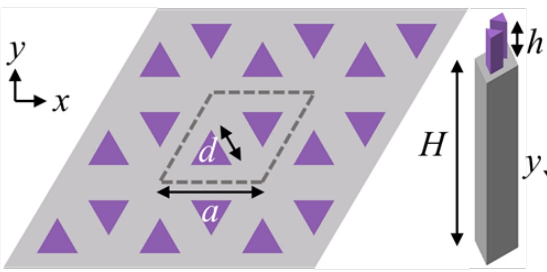

Breaking the inversion symmetry

Keeping the C_3 symmetry

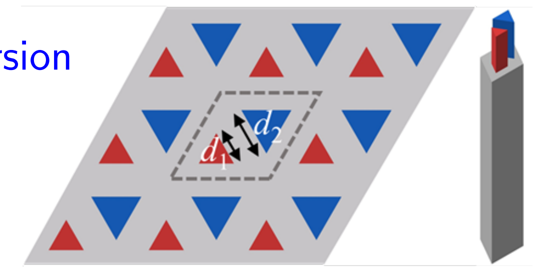

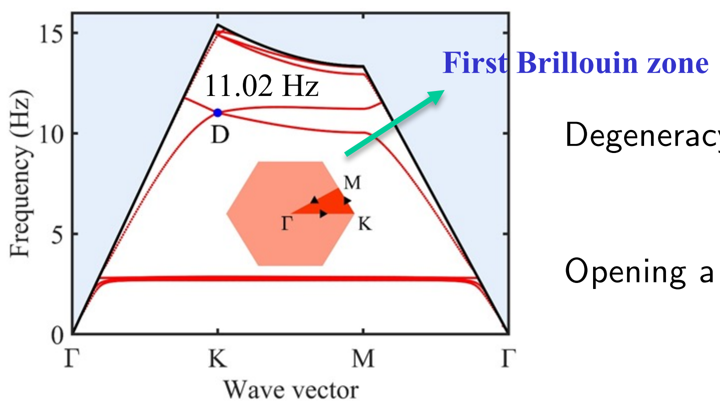

Degeneracy of the Dirac point

Opening a non-trivial bandgap

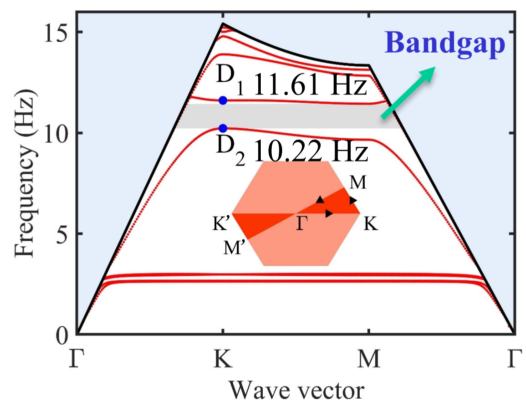

a(m)	d(m)	d_1(m)	d_2(m)	h(m)	H(m)
2.0	0.8	0.7	0.8	2.0	30.0

Topological edge states

- A point source out-of-plane vibration is excited at the entrance of the zig-zag interface for transmission calculation.
- With the electro-mechanical coupling effect, the vibrating energy can be transformed to electric power by the squire PZT patches attached to the top surface of soil.

- A simple circuit powered by each PZT patch with a resistance R is devised, whose average output power P_i is calculated by

$$P_i = \frac{V_i}{\sqrt{2}}\frac{I_i}{\sqrt{2}} = \frac{RI_i^2}{2}$$

The total power $P = \sum_{i=1}^{5} P_i$

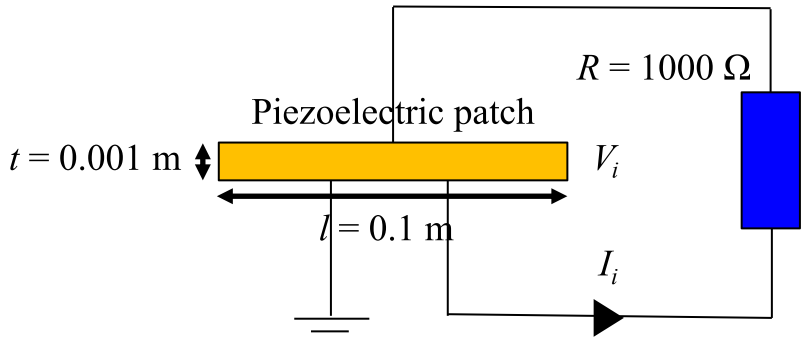

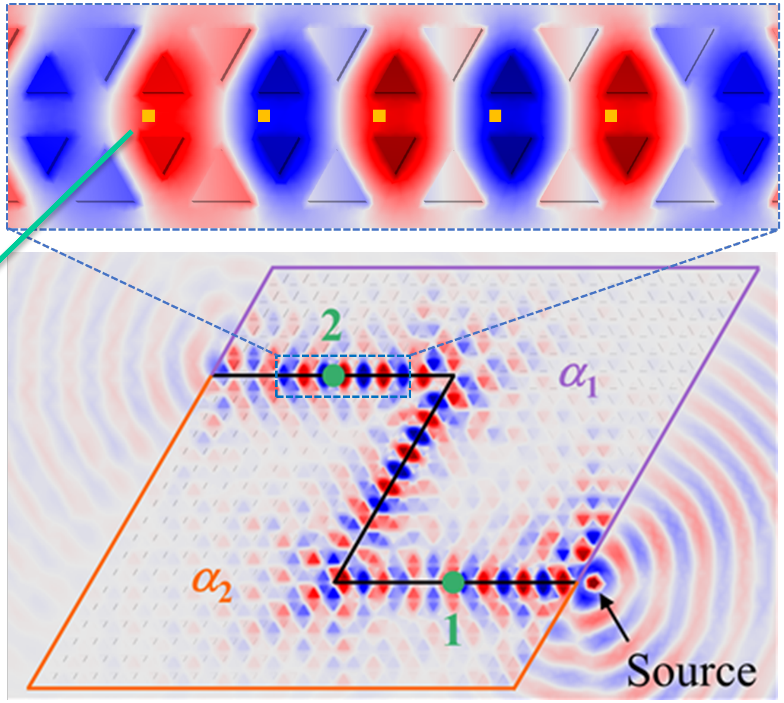

Topological edge states

- **The topological edge state within the frequency range (10.33, 10.97) Hz.**
- At 10.40 Hz, the S-S interface supports high transmission and backscattering immunity of the topological edge state.
- It is more than **one order of magnitude higher than that of a bare surface**, showing a big advantage of the energy harvesting by topological edge state.

Piezoelectric energy harvesting for the edge states

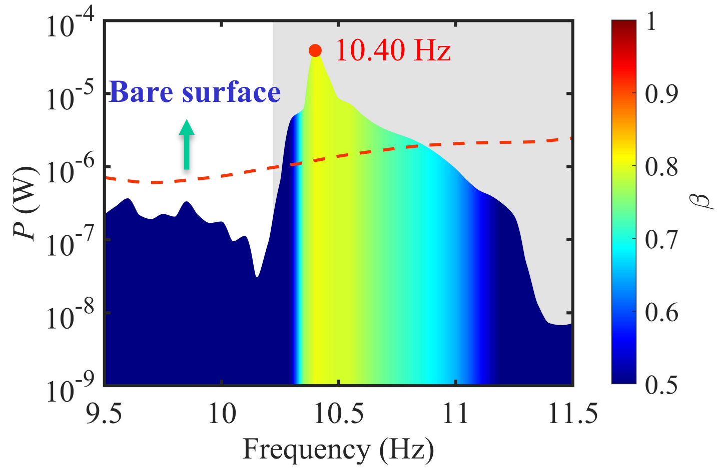

Out-of-plane displacement fields at 10.40 Hz

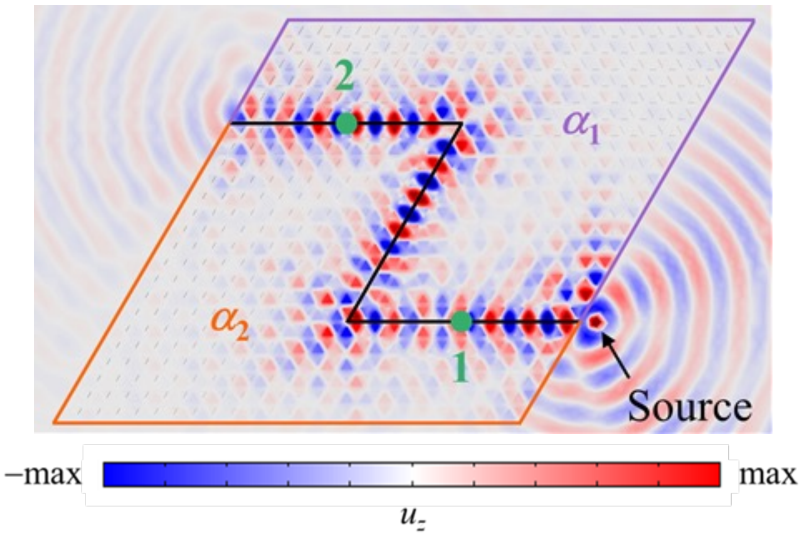

On demand design of phononic MM

Review

Yabin Jin*, Liangshu He, Zhihui Wen, Bohayra Mortazavi, Hongwei Guo, Daniel Torrent, Bahram Djafari-Rouhani, Timon Rabczuk, Xiaoying Zhuang* and Yan Li*

Intelligent on-demand design of phononic metamaterials

https://doi.org/10.1515/nanoph-2021-0639
Received October 28, 2021; accepted December 14, 2021; published online January 4, 2022

Abstract: With the growing interest in the field of artificial materials, more advanced and sophisticated functionalities are required from phononic crystals and acoustic metamaterials. This implies a high computational effort and cost, and still the efficiency of the designs may be not sufficient. With the help of third-wave artificial intelligence technologies, the design schemes of these materials are undergoing a new revolution. As an important branch of artificial intelligence, machine learning paves the way to new technological innovations by stimulating the exploration of structural design. Machine learning provides a powerful means of achieving an efficient and accurate design process by exploring nonlinear physical patterns in high-dimensional space, based on data sets of candidate structures. Many advanced machine learning algorithms, such as deep neural networks, unsupervised manifold clustering, reinforcement learning and so forth, have been widely and deeply investigated for structural design. In this review, we summarize the recent works on the combination of phononic metamaterials and machine learning. We provide an overview of machine learning on structural design. Then discuss machine learning driven on-demand design of phononic metamaterials for acoustic and elastic waves functions, topological phases and atomic-scale phonon properties. Finally, we summarize the current state of the art and provide a prospective of the future development directions.

Keywords: 2D materials; hierarchical structure; inverse design; machine learning; metamaterials; phononic crystals.

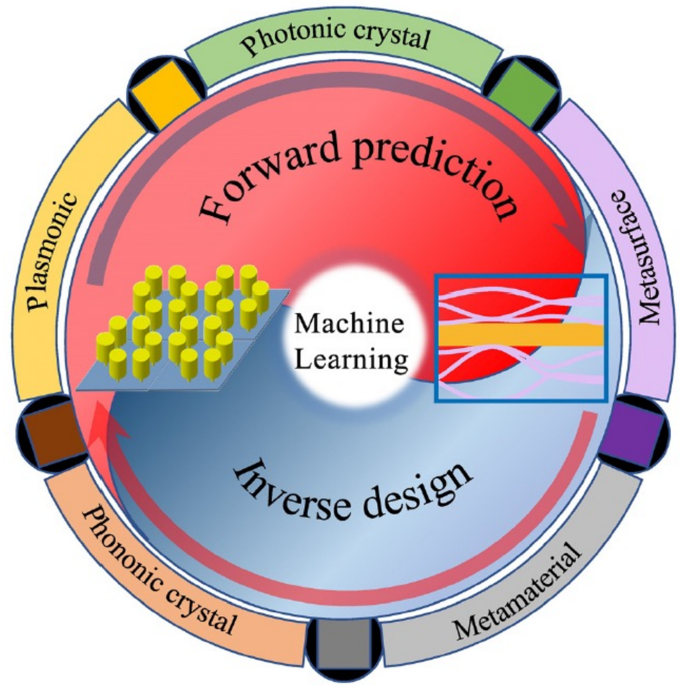

Thank you your attention

Thanks to Timon Rabczuk, Harold Park, Subbiah Nanthakumar, Bo He, Javvaji Brahma, Bin Li, Hamid, Ghasemi, Mortarzavi Bohayra, Ranran Zhang, Binh Huy Nguyen, Chuong Nguyen, Hongwei Guo, Tran Quoc Thai, Patrico Rodroguiz.

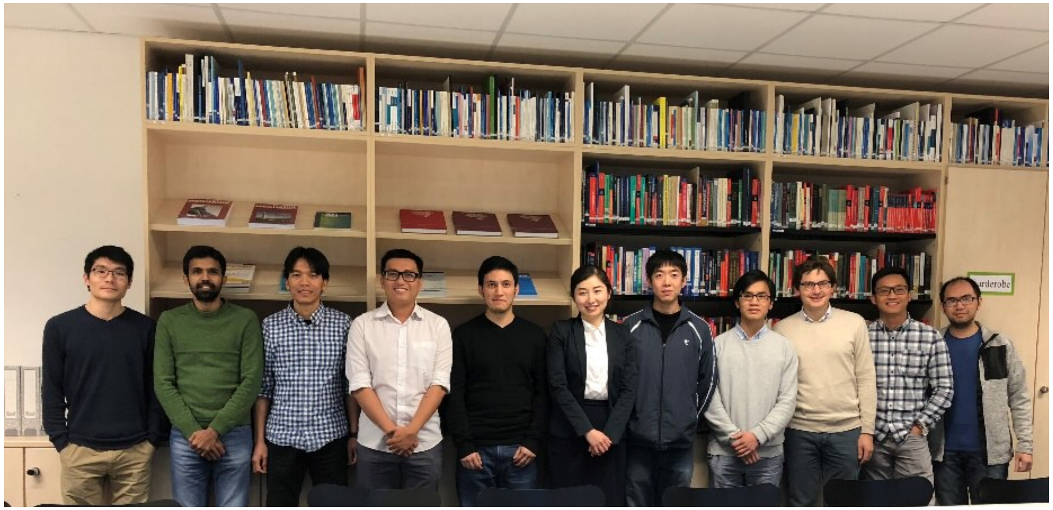

European Research Council
Established by the European Commission